The Structure and Function of the TACC Protein Family in Neurodevelopment

Author: Matt Evans

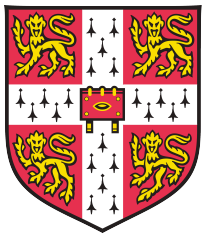

The Structure and Function of the TACC Protein Family in Neurodevelopment

Matthew Evans
Lowery Lab, Boston College
Holt Lab, University of Cambridge

Senior Thesis, May 2015
Biology Honors Program
Scholar of the College Program

Laura Anne Lowery, PhD, Advisor
Boston College Biology Department
140 Commonwealth Avenue, Chestnut Hill, MA 02467

TABLE OF CONTENTS

ACKNOWLEDGEMENTS

I owe the deepest gratitude to Dr. Laura Anne Lowery of Boston College for the incredible opportunity she gave me when I joined the lab, and her years of priceless mentorship and guidance. I also thank Anna Faris and Belinda Nwagbara for their illustrious instruction and patience in training me when I first joined the lab in October of 2013. I'd also like to thank Burcu Erdogan, Beth Bearce, Chris Lucaj, Patrick Ebbert and Joey Volk for their collaboration and assistance with these experiments. The entire Lowery Lab will always hold a dear place in my heart for my years spent here.

Further gratitude is due to Dr. Christine Holt of the University of Cambridge for enabling my research there, as well as Dr. Vasja Urbancic, Hovy Wong, and the rest of the Holt/Harris for teaching me many invaluable research techniques, assisting me in my various experiments, and for providing a warm and welcoming community that I shall always remember. Finally, I would like to thank Dr. Danielle Taghian for her amazing friendship and mentorship over the years I have been at Boston College. She and the rest of the BC Biology Department have helped allow me to reach for my greatest potential.

ABBREVIATIONS USED

+end	Microtubule plus-end
AAK	Aurora A Kinase
Abl	Abelson Kinase
CCD	Charge-coupled device
cDNA	complementary DNA
Cdk1	Cyclin-dependent kinase 1
d-TACC	drosophila Transforming Acidic Coiled-Coil
EB1	plus-End Binding Protein 1
eIF4E	eukaryotic Initiation Factor 4E
EST	Expressed Sequence Tag
CLASP	Cytoplasmic Linker-Associated Protein 1
GC	Growth Cone
GFP	Green Fluorescent Protein
GSK-3ß	Glycogen synthase kinase 3 beta
KD	Knockdown
kDa	kiloDalton
MBS	Modified Barth's Saline solution
MMR	Marc's Modified Ringer's solution
MO	Morpholino
mRNA	messenger Ribonucleic Acid
MT	Microtubule
OE	Overexpression
PCR	Polymerase Chain Reaction
pCS2+	expression vector plasmid
PKA	Protein Kinase A
RFP	Red Fluorescent Protein
RGC	Retinal Ganglion Cell
rtPCR	reverse transcriptase Polymerase Chain Reaction
SDM	Site-Directed Mutagenesis
Ser	Serine
TACC	Transforming Acidic Coiled-Coil
TACC1	Transforming Acidic Coiled-Coil Protein 1
TACC2	Transforming Acidic Coiled-Coil Protein 2
TACC3	Transforming Acidic Coiled-Coil Protein 3
+TIP	+end-Tracking Protein
Thr	Threonine
Tyr	Tyrosine
XMAP215	*Xenopus* Microtubule-Associated Protein (215 kilodaltons)

ABSTRACT

The growing axon tip of a developing neuron is called a growth cone. In order to form the exact synaptic connection required for proper neurological function, the growth cone hosts an orchestra of hundreds of different genes and proteins interacting with extracellular cues to steer growth in the right direction. Mutations in genes required for this process are associated with many neurodevelopmental disorders and deficits in damage repair.

The goal of our current research is to study several of the components of this pathway, known as the TACC family members. Our data shows that TACC1 and TACC3 are both present in the nervous system of developing embryos, and that knocking down TACC3 changes microtubule polymerization dynamics, altering the rate of growth and steering of the axon. Additionally, we have shown TACC3 to be one of a family known as +end-tracking proteins (+TIPs), protein complexes that bind the +end of microtubules to regulate their behavior, and have preliminary data that TACC1 behaves similarly. Therefore we believe the TACC family members are key players in neural development by regulating microtubule dynamics.

Here, we present a detailed structure/function analysis of the TACC family in regards to binding and activity with other proteins in the growth cone. We investigate the function of TACC3 in mediating neuron outgrowth and guidance *in vivo*. We examine which domains and specific amino acid residues mediate TACC function in regulation of cytoskeletal growth. We have found that the coiled-coil domain of the TACC family is necessary for its +end binding activity, and certain amino acid residues upstream of and within this domain enable the activity of TACC3. We believe these residues and their

phosphorylation-based regulation facilitates the binding of TACC3 to other +end proteins and the +end itself, and that this process enables the regulated polymerization of microtubules and growth of the developing neuron. Studying this process and the role of the TACC family overall will help provide a powerful model for understanding the function of genes involved in cytoskeletal regulation and neurodevelopment.

Chapter I: Introduction

TACC3 and the Growth Cone

Growth Cones and Neurodevelopment

Throughout the process of neurodevelopment, the cytoskeleton of cells within the nervous system is dynamically regulated in order to ensure proper growth and migration (Lowery and Van Vactor, 2009). There are a vast number of genes involved in this process, which function together to grow, rearrange, destroy, and regrow the cytoskeleton to facilitate certain structural changes and migrations of the cell. Perhaps the most intriguing example of this phenomenon occurs in the growing tip of a developing neuron axon – the growth cone.

The growth cone is a hand-like structure that splays out at the tip of a growing axon. It grows out from the soma (body) of the neuron and probes the environment of the cell's surroundings. By integrating a host of extracellular guidance cues and genetic factors, the growth cone weaves its way throughout the developing brain to find its correct synaptic target. Many of the genes involved in the guidance process are critical for proper nervous system development; mutations often result in developmental disorders and neuropathologies (Engle *et al*., 2010; Tischfield *et al*., 2010). Some of these genes deal with processing extracellular guidance signals and growth factors, some relay these signals to effector genes, and some enact the signal by changing the dynamics of the cellular skeleton within the growth cone.

Cytoskeleton and +TIPs

Within the growth cone, a number of dynamic cytoskeletal factors interact to ensure the proper growth and guidance of the axon tip. Key elements of these factors are microtubules (MTs) and the protein complexes that lie on the growing +ends of microtubules. These proteins are known as +TIPs, or +end-tracking proteins. +TIP

proteins regulate the growth of microtubules (Akhmanova and Steinmetz, 2008) in a carefully coordinated way so as to ensure proper cytoskeletal formation and dynamics. The +TIPs present in growth cones help to ensure proper development and growth of the axon (Tanaka *et al*., 1995; Lowery and Van Vactor, 2009).

Within the growth cone, most of the microtubules are stable and confined to the central domain, the "wrist" of the metaphorical hand (Figure 1). These microtubules are stabilized and serve to support the developing axon. Some microtubules, however, probe out into the periphery in filopodia, and are dynamically regulated by +TIP proteins on their +ends. These dynamic microtubules will either grow or shrink in response to extracellular signals, called guidance cues. When more of these dynamic microtubules are stabilized on one side of the growth cone, it will steer in that direction, and when more are destabilized on one side, it will steer in the other direction (Tanaka *et al.,* 1995). Regulation by +TIPs is widely believed to be the determinant of these dynamic microtubule behaviors, and thus the growth and steering of the developing axon.

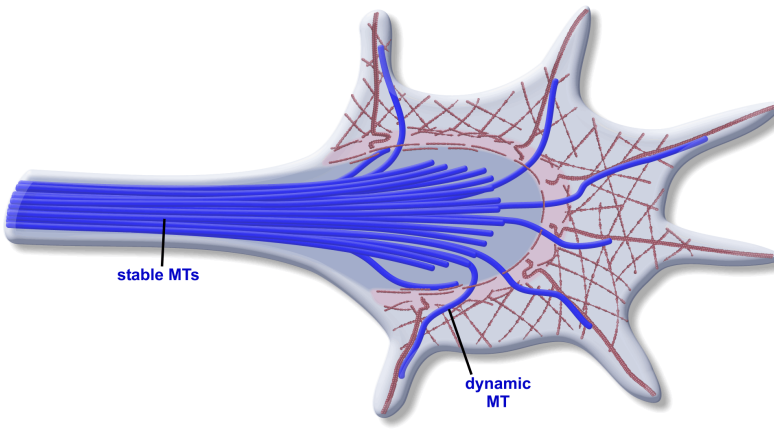

Figure 1: Growth Cone Cytoskeletal Proteins. Microtubules (MTs) depicted in blue, and actin filaments depicted in red. (Lowery and Van Vactor, 2009).

It remains poorly understood exactly how most +TIPs function with regards to their activity on the microtubule and interaction with each other. Furthermore, very few studies have examined how +TIPs function in vertebrate growth cones (e.g., van der Vaart *et al*., 2012; Lowery *et al*., 2013; Marx *et al*., 2013). Understanding how +TIPs regulate microtubule dynamics will help elucidate the phenomena of growth cone

guidance, which is key to understanding nervous system development. An analysis of the structure, function, and regulation of several of the key +TIPs will begin to explain this entire process.

Guidance Cues

The growth cone is guided to its correct synaptic target by a plethora of different signals known as guidance cues. These include the substrate it is growing on, other cells, axons, and growth cones around it, and diffusible peptide or protein. Receptors on the cell membrane of the growth cone bind to these guidance cues and relay a signaling cascade through the cytoplasm, which leads to an effect on the cytoskeleton (Campbell, 2001). Positive guidance cues will translate to stability of cytoskeletal edifices, increased polymerization rates, or synthesis of new cytoskeletal protein to push growth in that direction (Leung *et al.,* 2006). Guidance cues will determine which microtubules will be more

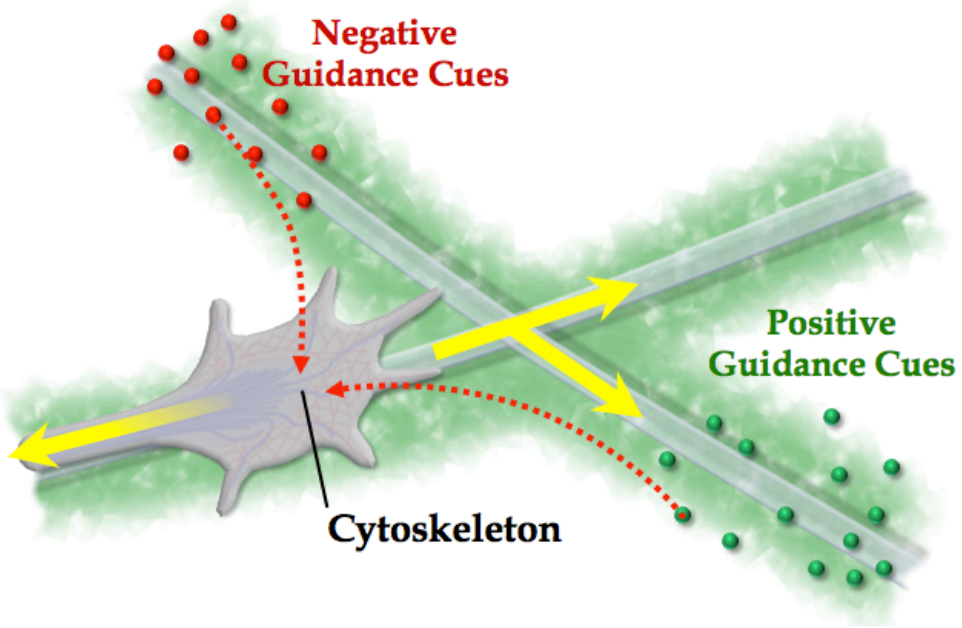

Figure 2: The Growth Cone Integrates Guidance Cues to affect cytoskeletal dynamics and steer axonal growth. (Modified from Lowery and Van Vactor, 2009).

stabilized and grow, which in turn will determine which way the developing axon steers itself (Figure 2).

Most guidance cues are expressed in varying levels in a specific part of the brain, at a specific developmental stage. Neurons originating from a specific cell type will express a certain type of receptor, and will respond to a localized guidance cue in a unique way when its growth cone reaches that part of the brain. A well-characterized model of this phenomenon is that of development of the optic nerve in the African Clawed Frog, *Xenopus laevis* (van Horck *et al.,* 2004). In this model (Figure 3), the retinal ganglion cell (RGC) departs the retina by following a positive, attractive gradient of Netrin-1 (green). Once it reaches the optic chiasm, the repulsive signal Ephrin-B enables sorting of the neurons based on which side of the retina they originated from. The negative cues Sema3A and Slit help steer it further until it reaches its destination in the optic tectum, where once again the neurons are repelled away from improper synaptic targets by Ephrin-B. This model, developed by the Holt/Harris labs of the University of Cambridge, presents a powerful means of assaying the relative ability of neurons to process a diversity of guidance cues and steer accordingly.

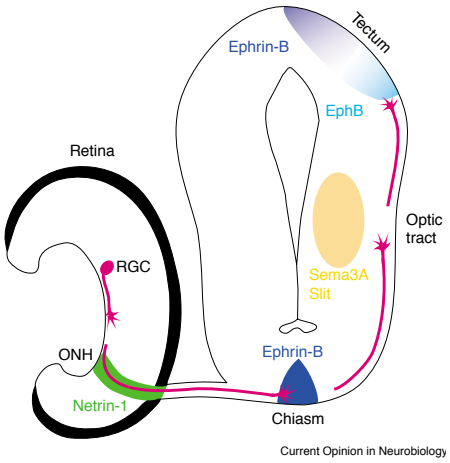

Figure 3: Retinal Ganglion Cell (RGC) Outgrowth (van Horck *et al*., 2004).

XMAP215 and other +TIPs

A number of +TIPs have been well-studied in other systems besides the growth cone, and their known functions make them likely to be critically important to the growth cone-guiding process. These include XMAP215, EB1, and CLASP (Akhmanova and

Steinmetz, 2008). XMAP215 is the most distally located +TIP on the microtubule and is a microtubule polymerase (Nakamura *et al*., 2012; Maurer *et al*., 2014). XMAP215 directly polymerizes microtubules, adding tubulin subunits to the growing +end. EB1 is another well-characterized +TIP (Honnappa *et al*., 2009) that binds the microtubule +end and provides a good marker for studying other +TIP localization.

CLASP is another +TIP that regulates microtubule dynamics in growth cones (Hur *et al*., 2011, Marx *et al*., 2013). It does this in response to the activity of certain signaling kinases, such as GSK-3ß (Hur *et al*., 2011) or Abelson (Abl) Kinase (Engle *et al.,* 2014). These kinases relay signals from extracellular cues to regulate microtubules within the growth cone and grow/steer it in the proper direction (Lee *et al*., 2004). Pictured below is the process by which extracellular guidance signals are translated by signaling kinases through the growth cone membrane, to elicit phosphorylation of CLASP and potentially other +TIPs. This, in turn, regulates microtubule dynamics in such a way to enable axon outgrowth and steering. Understanding the role of other +TIPs that CLASP and XMAP interact with will help elucidate the mechanism by which this regulation takes place.

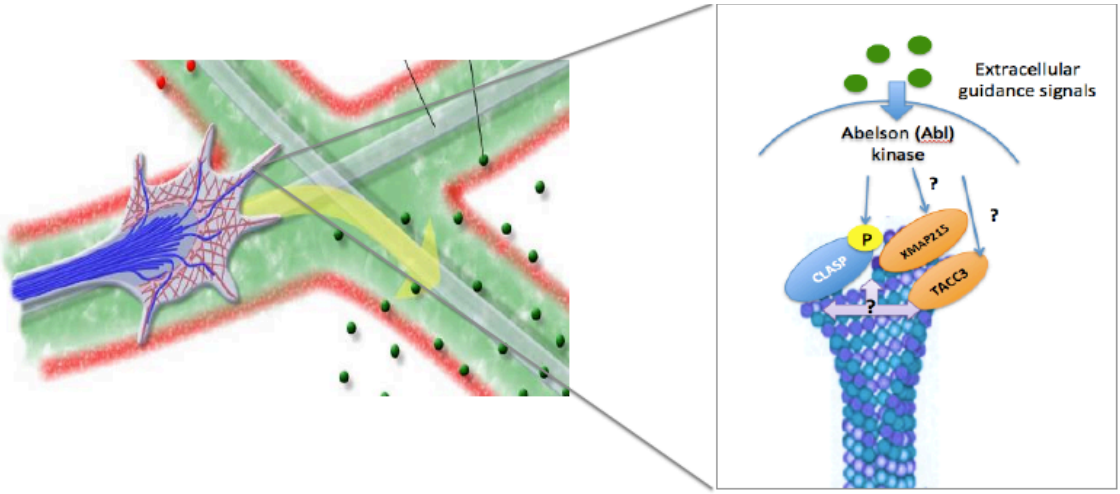

Figure 4: Guidance Cues and +TIPs. The growth cone processes guidance cues through signaling cascades that lead to phosphorylation of CLASP and possibly other +TIPs. (Modified from Lowery and Van Vactor, 2009).

In order to investigate the role of this protein complex in axon outgrowth and microtubule regulation as a whole, a multi-parametric analysis of the interaction partners of CLASP was done (Lowery *et al*., 2010, Long *et al*., 2013) and identified several novel genetic interaction partners, most notably the protein TACC3 (transforming acidic coiled-coil #3). TACC3 is known to bind XMAP215 in other systems (Lee *et al*., 2001), and has been studied with regards to its role in microtubule dynamics during mitosis (Kinoshita *et al.,* 2005). These known functions made it a promising candidate for further investigation into the +TIP complex.

TACC3

TACC3 is one of the members of the Transforming Acidic Coiled-Coil domain family, and was first identified as a centrosomal-associated protein implicated in stabilizing microtubules during mitosis (Gergely *et al*., 2000a; Peset and Vernos, 2008). Immunostaining experiments had demonstrated its additional presence on microtubules within the centrosome and the mitotic spindle (Groisman *et al*., 2000). Knockdown experiments, done to reduce the amount of protein made within the living cells of an organism, have shown that reduced TACC3 levels lead to reduced microtubule length in astral and spindle microtubules formed during mitosis in several animal models; worms (Bellanger and Gonczy, 2003; Le Bot *et al*., 2003; Srayko *et al*., 2003), flies (Gergely *et al*., 2000b), and vertebrate cells (Kinoshita *et al*., 2005; O'Brien *et al*., 2005; Peset *et al*., 2005). On the other hand, increasing levels of TACC3 through artificially introducing high mRNA levels into the cells leads to the formation of longer mitotic spindles (Gergely *et al*., 2000a; Peset *et al*., 2005). These results implicate TACC3 as a microtubule stabilizing or growth-promoting factor.

As TACC3 is known to bind and interact with XMAP215 (Lee *et al*., 2001) it was suggested that TACC3 could be recruiting XMAP215 to the centrosome during mitosis, to enable creation or help in polymerizing mitotic spindle and astral microtubules (Peset and Vernos, 2008). Studies analyzing the interaction of TACC3 and XMAP215 showed that TACC3 does localize XMAP215 to the centrosome, and that this interaction is essential for proper mitotic spindle assembly (Lee *et al*., 2001; Kinoshita *et al*., 2005; O'Brien *et al*., 2005; Peset *et al*., 2005). While XMAP215 is also a well-known +TIP (Brouhard *et al.*, 2008), it was unclear if this interaction with TACC3 is also necessary for its activity on +ends of microtubules during interphase.

A study done in *Drosophila* found that the TACC3 homolog d-TACC, the only TACC family member present in the fly model, did localize in small puncta emanating from the centrosome, indicating its nature as a +TIP (Lee *et al.,* 2001). However, no further studies of TACC family members as +TIPs had been done by the time of the beginning of this study.

TACC3 has attracted interest in other realms besides microtubule dynamics, particularly the field of neuronal development. TACC3 is enriched in the developing embryonic nervous system of *Xenopus laevis* (African Clawed Frog) embryos (Tessmar *et al*., 2002), as well as being up-regulated when PC12 cells differentiate into neurons (Sadek *et al*., 2003). Additionally, TACC3 helps to maintain the pool of neural progenitor cells differentiating to various nervous system cell lines during neocortical development (Xie *et al*., 2007). TACC3 is necessary for the neurogenesis of radial glial cells in the neocortex into new neurons (Yang *et al*., 2012). Overall, it is clear that TACC3, in addition to its functions as a microtubule-associated protein involved in mitosis, is highly important for the development of the nervous system specifically.

TACC3 is a +TIP

Our lab set out to study the role of TACC3 within the growth cone. We investigated the localization of fluorescent-labeled TACC3 within the growth cone of developing neurons, as well as in other embryonic cell types, including cultured embryonic neural crest cells. We also did knockdown (KD) and overexpression (OE) experiments, to reduce and increase (respectively) the amount of TACC3 protein present in the cell. Through these techniques we were able to quantify the effects of these manipulations on various parameters of neurodevelopment, such as the number of axons that successfully grow out, and the length of the resulting axons. We also computed TACC3's effects on microtubule dynamics through software-based processing of time-lapse images of the +TIP EB1 tracking microtubule +ends in live growth cones subject to TACC3 knockdown or overexpression.

Our lab's work clearly demonstrated that TACC3 is a +TIP in growth cones (Figure 5), as well as in other *Xenopus* embryonic cell types (not pictured) such as neural crest cells and mesenchymal fibroblast cells (Nwagbara *et al*., 2014). In these initial localization experiments it was confirmed that TACC3 is a member of the +TIP family and decorates the tips of dynamic microtubules within live growth cones.

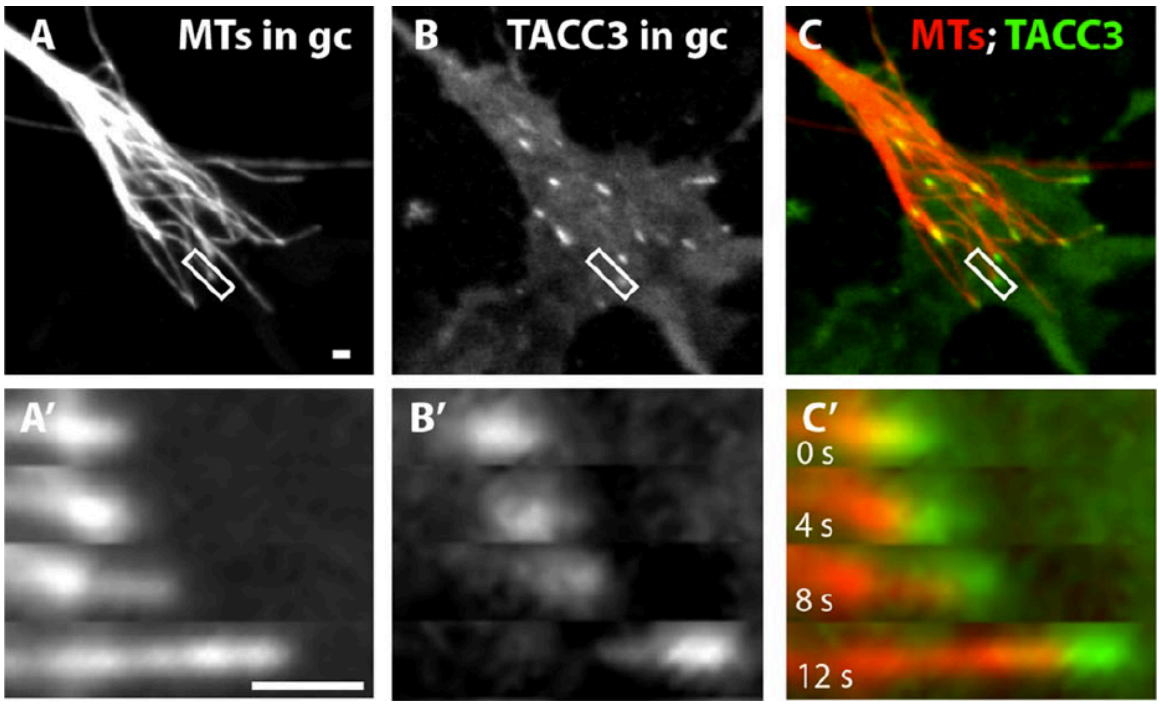

Figure 5: TACC3 is a +TIP in Growth Cones
Fluorescence time-lapse imaging of cultured neuron growth cones expressing fluorescent-tagged GFP-TACC3 (green) and mkate2-tubulin (red). (Nwagbara *et al*., 2014, Figure 3A-C).

Further analysis of the localization of TACC3 highlighted a unique characteristic of its +TIP nature. When the GFP-tagged fluorescent TACC3 construct was imaged alongside a red fluorescent construct of the well-characterized +TIP EB1, TACC3 appears more distally located on the +end of the microtubule (Figure 6, left). When a red fluorescent TACC3 construct was imaged alongside a green fluorescent construct XMAP215, which resides on the *very* tip of the +end, it appears to co-localize perfectly on top of XMAP215 (Figure 6, right). These data indicate that TACC3's role in the +TIP complex is likely heavily involved with XMAP215, as the two proteins are known to interact in other vertebrate cell systems, albeit during mitosis. TACC3's job may be to help recruit or regulate XMAP215 in regards to its function in polymerizing microtubules.

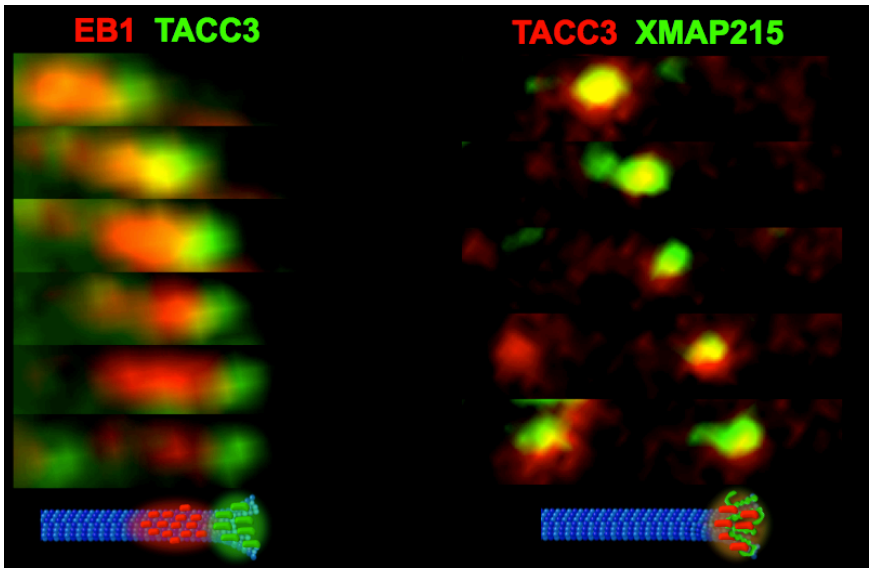

Figure 6: TACC3 is on the very tip of growing MTs, co-localized with XMAP215
Left: Fluorescent time lapse images of green fluorescent GFP-TACC3 on the growing +end of a microtubule, co-localized in front of red fluorescent mkate2-EB1
Right: Fluorescent time lapse images of red fluorescent mkate2-TACC3 on the growing +end of a microtubule, co-localized with green fluorescing GFP-XMAP215. Cartoon images below demonstrate MT localization. (Nwagbara et al., 2014 Figure 6C, G)

To further examine the presence of TACC3 so perfectly aligned with XMAP215, we performed statistical behavior assays of the microtubules present in the growth cone (Figure 7). We determined that virtually ALL of the microtubules that were in the process of polymerizing (growing) had TACC3 present on the +TIP, whereas only most of the ones that had paused their polymerization still had TACC3 present, and few of the actively depolymerizing (shrinking) ones had any TACC3 present on the +TIP.

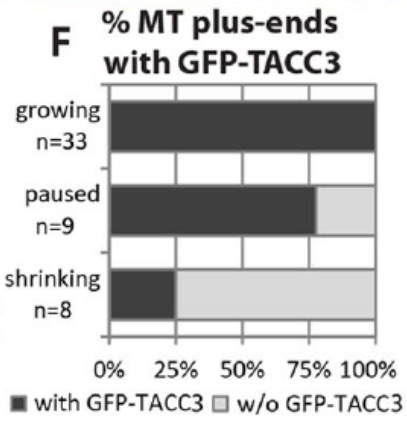

Figure 7: TACC3 is mostly on growing +ends
Quantification of microtubule time-lapse imaging revealed the distribution of TACC3 on microtubule +ends depending on their polymerization rate at the time. (Nwagbara *et al*., 2014 Figure 3F).

These data further indicated that TACC3's presence on the +TIP may serve to recruit XMAP215 and regulate its function so as to enable microtubule polymerization. This would, in turn, enable dynamic regulation of microtubules in the growth cone periphery based on the behavior of TACC3 itself.

Now that we understood where TACC3 localizes within the growth cone, and how it binds the very tip of the +TIP alongside XMAP215, it was possible to develop a model for TACC3's function in axon outgrowth. A growth cone is depicted here (Figure 8) with

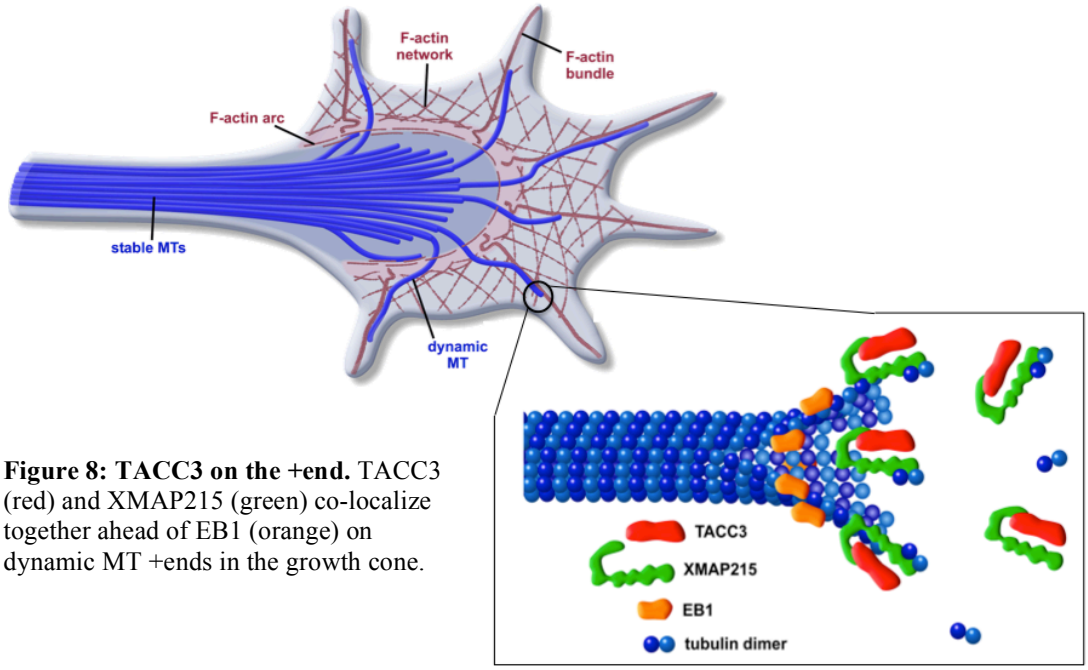

Figure 8: TACC3 on the +end. TACC3 (red) and XMAP215 (green) co-localize together ahead of EB1 (orange) on dynamic MT +ends in the growth cone.

a highlighted dynamic microtubule +TIP probing the growth cone periphery in a regulated way. It is likely that TACC3 plays a significant role in the regulation of these dynamic microtubules, probably through its regulated interaction with XMAP215. TACC3, therefore, would be a critical player in the entire process of axon outgrowth and steering. In order to further understand the role of TACC3 in neuron growth and guidance, however, we first had to determine what is it doing on the +ends of microtubules in the first place.

TACC3's Role in the +TIP Complex

To begin to explore the role of TACC3 in neurodevelopment, we first evaluated the effects of its presence on the +end of microtubules within the growth cone. Most

+TIPs regulate microtubule dynamics in some way or another (Akhmanova and Steinmetz, 2008). Therefore we predicted TACC3 to have some kind of regulatory effect on the microtubules it bound. We performed a series of knockdown (KD) and overexpression (OE) experiments to manipulate TACC3 protein levels artificially to compare microtubule behavior when TACC3 protein levels are normal (control) reduced (TACC3 KD) or increased (TACC3 OE).

We observed and quantified the effects of these genetic manipulations on microtubules by analyzing the tracks of fluorescent EB1 protein using the MATLAB-based software +TIP Tracker. This program efficiently tracks the fluorescent signal of EB1 tracking the growing end of microtubules and computes their growth velocity, growth duration, and growth length. These data (Figure 9) demonstrated that TACC3 has

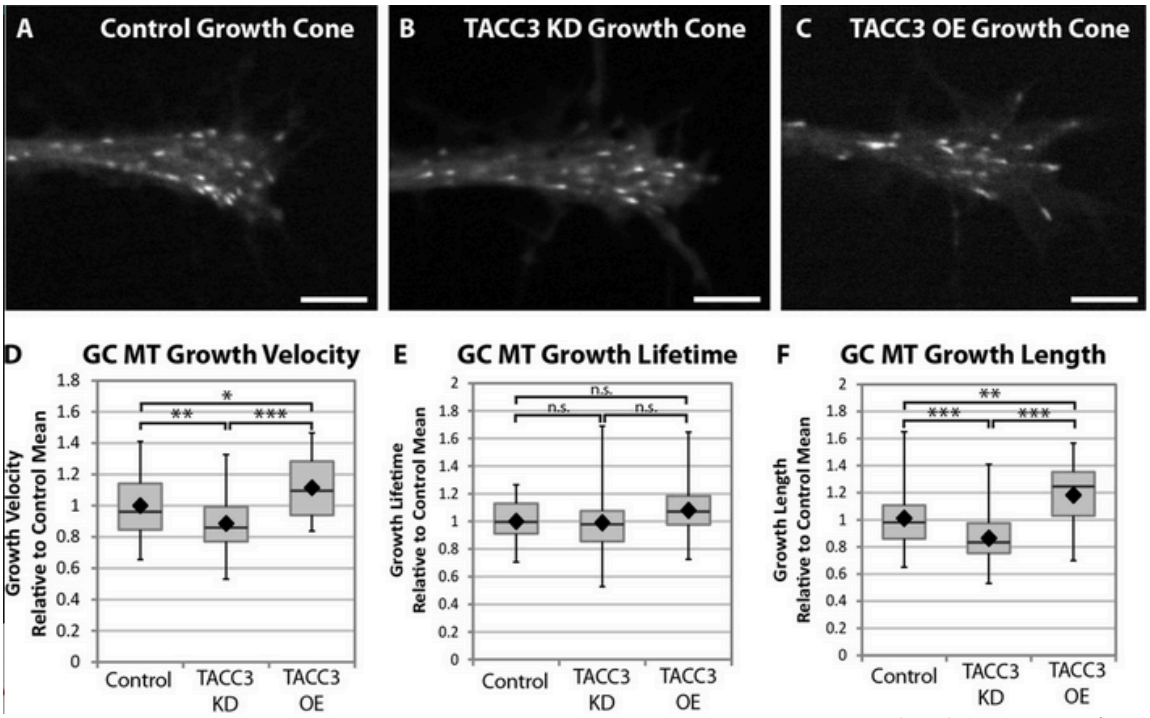

Figure 9: TACC3 increases MT growth velocity and length, but not lifetime. (A-C): Representative images of EB1-GFP comets in control (A), TACC3 KD (B), and TACC3 OE (C) conditions. Bar, 5 μm. (D–F): Quantification of MT growth track parameters in cultured growth cones (GC) after TACC3 manipulation. EB1-GFP localizes to the ends of growing MTs and is thus a marker for MT polymerization. Automated tracking of EB1-GFP comets calculate MT growth-track velocity (D), MT growth-track lifetime (E), and MT growth-track length (F). An unpaired t test was performed to assess significance of over-expression conditions compared to control. ***p<0.001, ****p<0.0001; n.s., not significant. (Nwagbara *et al.,* 2014, Figure 2 A-F).

a significant effect in promoting increased microtubule growth velocity, increased length of microtubule growth. It does not, however, increase the length of time the microtubule is growing. Taken together with TACC3's co-localization with XMAP215, these data indicate that TACC3 binding the +end with XMAP leads to more effective microtubule polymerization enacted by XMAP. While this interaction would not necessarily stabilize the polymerizing microtubules (therefore increasing its growth lifetime) it would lead to faster growth, and therefore a longer total growth in the same time period.

Having determined the effect of TACC3 on the +ends of dynamic microtubules in the growth cone, we then sought to determine if and how this effect translates to an overall role in neuronal development. To further explore how exactly TACC3 may influence neuron development and growth, we performed another series of TACC3 knockdown (KD) experiments. Injecting TACC3 morpholino into developing embryos, combined with neuron culturing techniques, allowed us to observe neuron development and growth *in vitro* so that we could observe any resultant phenotypic effects due to insufficient TACC3, such as changes in the ability of axons to grow out. Further KD experiments done in conjunction with electroporation and live embryo imaging techniques enabled studying neuron development and growth *in vivo* so we could replicate the findings of the *in vitro* studies in a more accurate representation of actual neurodevelopment, as well as allowing us to study neuron guidance in a living system.

First, the *in vitro* effect of TACC3 KD was assayed through analysis of axon outgrowth, quantified through the number and length of axons cultured from neural tube explants. These experiments demonstrated a significant reduction of axon outgrowth in both means of quantification (Figure 10). We therefore hypothesized TACC3 to be

involved in the promotion of axon outgrowth, through increasing the ability of neurons to send out and maintain a growing axon, and to promote axon growth in general.

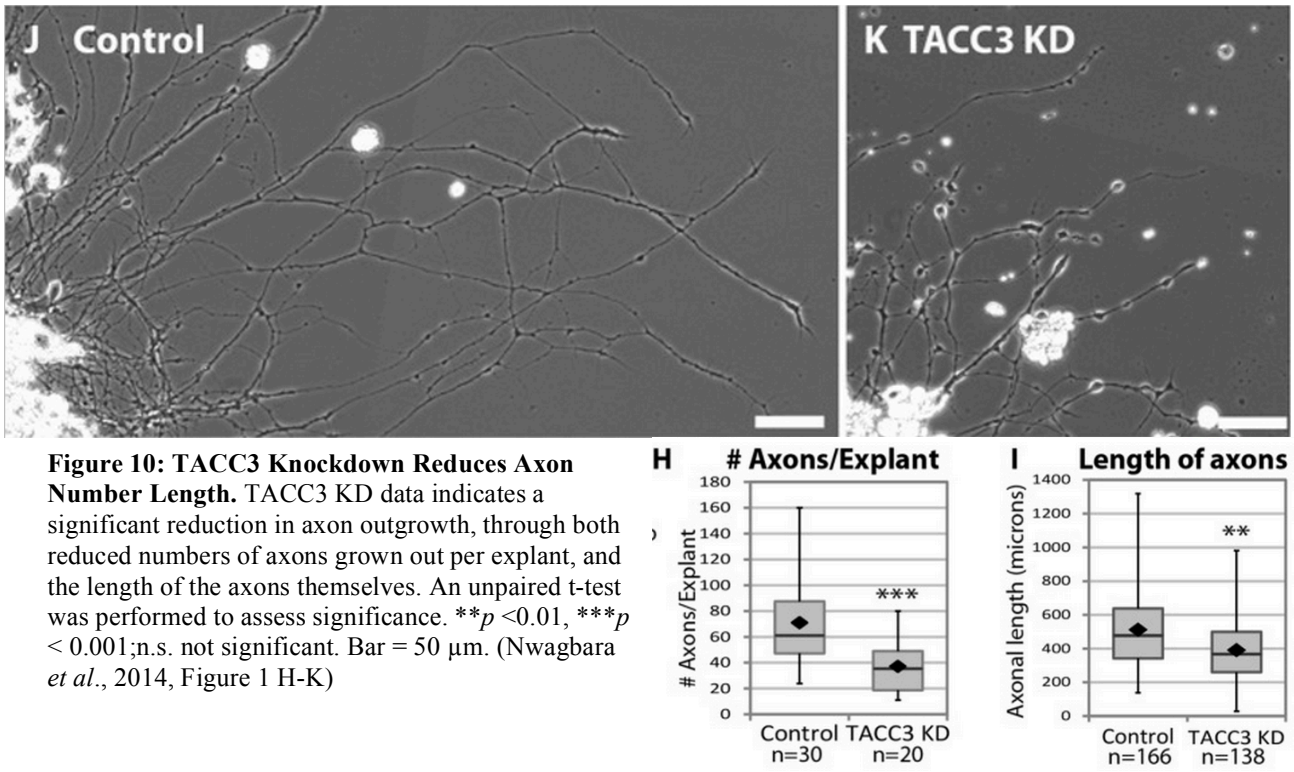

Figure 10: TACC3 Knockdown Reduces Axon Number Length. TACC3 KD data indicates a significant reduction in axon outgrowth, through both reduced numbers of axons grown out per explant, and the length of the axons themselves. An unpaired t-test was performed to assess significance. $^{**}p < 0.01$, $^{***}p < 0.001$;n.s. not significant. Bar = 50 µm. (Nwagbara *et al*., 2014, Figure 1 H-K)

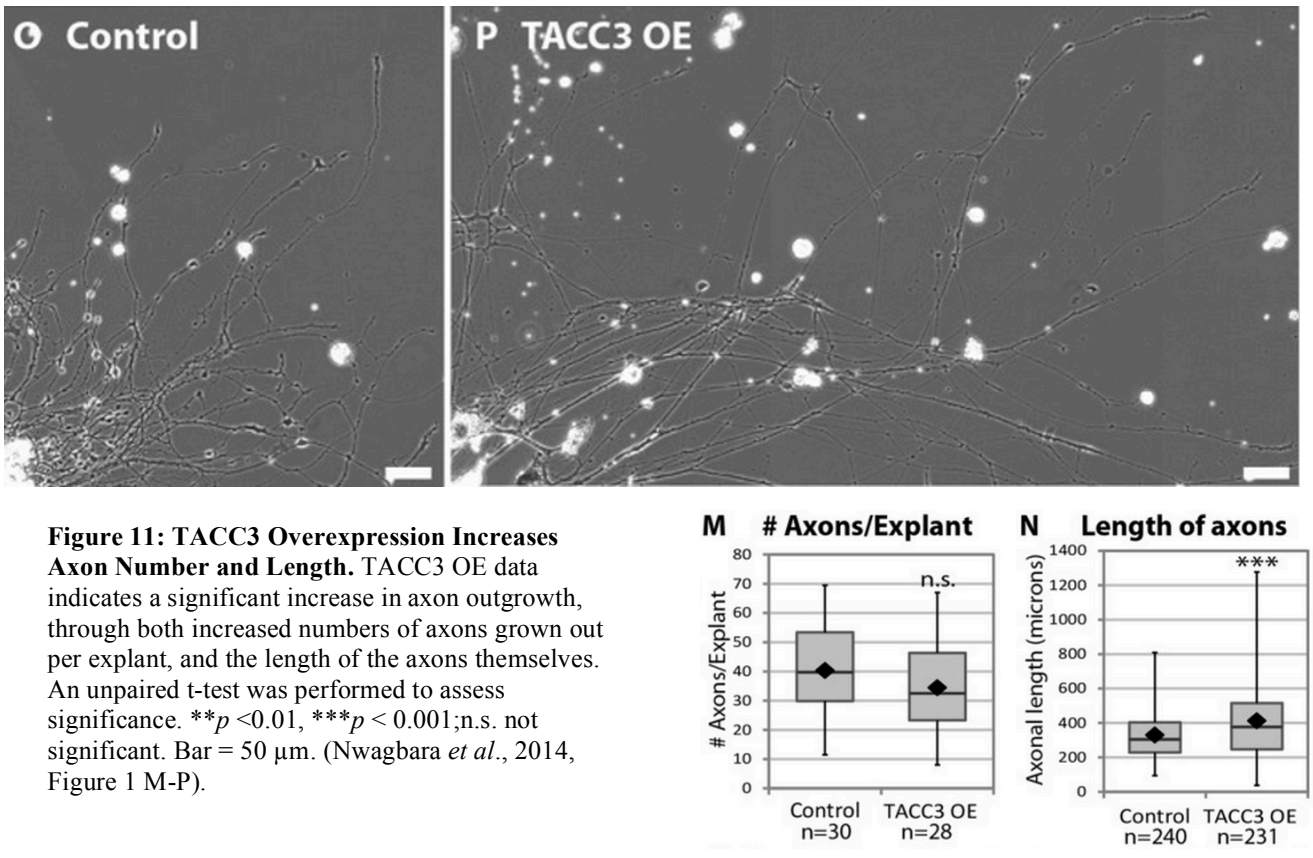

Figure 11: TACC3 Overexpression Increases Axon Number and Length. TACC3 OE data indicates a significant increase in axon outgrowth, through both increased numbers of axons grown out per explant, and the length of the axons themselves. An unpaired t-test was performed to assess significance. $^{**}p < 0.01$, $^{***}p < 0.001$;n.s. not significant. Bar = 50 µm. (Nwagbara *et al*., 2014, Figure 1 M-P).

We then sought to examine the effect of *increasing* TACC3 protein levels within neurons. We again performed overexpression (OE) experiments to raise levels of TACC3 protein within embryonic cells. The effects of this manipulation were quantified the same way as for the KD experiments and complement their findings (Figure 11). TACC3 was again shown to promote the length of axons growing out from neural tube explants. However, increasing the protein levels did increase the number of axons growing out.

Based on the findings of our lab described above, we hypothesized that TACC3 was enabling and regulating the activity of XMAP215 on the growing +ends of dynamic microtubules within the growth cone. This effect leads to a promotion of microtubule polymerization, which translates to promoting axon outgrowth in general. With insufficient TACC3, dynamic microtubules would be less able to grow out and explore the periphery to provide the tracks of further cytoskeletal growth. This would lead to slower and shorter axons, and in all likelihood more axonal retraction and death, explaining the reduced number of axons visualized in Figure 10.

The goal of this thesis originated as further investigation into the function of TACC3 in neurodevelopment. As TACC3 regulates dynamic microtubules within the growth cone, it is possible that it itself is regulated in response to guidance cues as a necessary component of enabling growth cone steering, warranting investigation of the effects of TACC3 on neuronal guidance. The regulation of TACC3 would likely be structural in nature, so understanding the structure of TACC3 itself and how it binds the +end and interacts with XMAP215 is another key component of this hypothesis. Additionally, as TACC3 shares many of its structural features with the other members of the TACC protein family, it became necessary to evaluate these other members for similar behaviors.

Chapter II: TACC3 and Neurodevelopment

Having demonstrated the significant effect of TACC3 in promoting axon outgrowth, my research sought to evaluate TACC3's potential effect on axon guidance. To study this, I obtained a grant to travel to the Holt lab at the University of Cambridge. The Holt lab has thoroughly characterized the guidance of retinal ganglion cells (RGCs) in developing *Xenopus* embryo brains, making their outgrowth an effective model for studying the ability of neurons to respond to guidance cues. They have also pioneered the development of a few powerful and specific means of manipulating, studying, and quantifying RGC guidance *in vivo.* At Cambridge, I performed two classes of experiments on TACC3. First, I sought to replicate the effects of TACC3 KD on RGCs themselves, to ensure that the effect of TACC3 KD is conserved in this model. Secondly, I investigated the *in vivo* guidance of these neurons in the developing brain.

MATERIALS & METHODS

Xenopus Embryos

Xenopus laevis embryos were fertilized through *in vitro* fertilization, dejellied, and cultured at 14-22^{o}C in 0.1x modified Barth's saline (MBS; 0.88 mM NaCl, 0.01 mM KCl, 0.024 mM $NaHCO_3$, 0.1 mM HEPES, 8.2 μM $MgSO_4$, 3.3 μM $Ca(NO_3)_2$, 4.1 μM $CaCl_2$). They were raised using standard methods (Sive *et al*., 2010) and staged as described in Nieuwkoop and Faber (1994). All animal experiments were approved by the University of Cambridge Local Ethical Review Committee.

Culture of Xenopus embryonic eye explants

Embryos were cultured in 0.1× MBS at 22°C to stages 30-32, and each eye primordial was dissected out and plated retina-side down in L15-derived culture medium

on poly-l-lysine (100 μg/ml)– and laminin (20 μg/ml)-coated coverslips attached to a plastic culture dish with a hole drilled in the center (imaging chambers described in Gomez *et al*., 2003). Outgrowing retinal axons were imaged at room temperature 24 h after plating.

Morpholinos

MOs targeted to the translation start site of *X. laevis* TACC3 (5′-AGT-TGTAGGCTCATTCTAAACAGGA-3′) or standard control MO (5′-cctcttacctcagttacaatttata-3′; purchased from Gene Tools [Philomath, OR]) were injected into two- to four-cell-stage embryos (80 ng/embryo). Protein knockdown was assessed by Western blot of embryos at stages 35–36. In rescue experiments, MO was injected along with mRNA in the same injection solution.

Electroporation

Embryos were cultured at 22^{o}C in 0.1X MBS to stage 28. The embryos were electroporated with membrane-targeted GAP-GFP or GAP-RFP fluorescent constructs as described in Falk *et al*., 2007. The embryos were held in a specially designed electroporation chamber in 1X MBS, and a solution containing 1 μg/μL of the desired fluorescent construct was injected into the third ventricle of the developing brain. Electroporation was performed immediately after injection with a IntraCel TSS20 Ovodyne Electroporator using 8 20V x 50 ms square-wave pulses to introduce the DNA into the retinal ganglion cells. Embryos were then allowed to develop in 0.1X MMR for another 24 hours, after which they were dissected according to the ventral brain prep protocol.

Ventral Prep of Electroporated Embryo Brains

Electroporation was performed on stage 28 embryos using the standard protocol. When reaching stage 39, embryos were anaesthetized in 0.05 mg/ml MS222/1× MBS and dissected as described in van Horck *et al.,* 2004. The skin covering the embryo head was removed, as well as the ventral section of the head to expose the ventral side of the brain. The head was then carefully separated from the body and placed in a well made from circular reinforcement labels (Avery, 5722) placed on an oxygen permeable slide (Permanox, Nalgen Nunc, 16005). Only samples with a few isolated axons were selected for subsequent live imaging. Image acquisition was performed on a Nikon Optiphot-2 microscope equipped with a 20× Plan NeoFluar objective and Orca-ER cooled CCD camera (Hammamatsu).

Live Imaging of Electroporated Axons *in vivo*

Electroporation was performed on stage 28 embryos using the standard protocol. When reaching stage 39, embryos were anaesthetized in 0.05 mg/ml MS222/1× MBS and prepared for live imaging as described in Dwivedy *et al.*, 2007. Briefly, the eye and skin covering the contralateral brain were removed to expose the transfected axons. The embryo head was placed in 0.05 mg/ml MS222/1× MBS filled chamber formed by a gene frame (ABGene, AB 0576) placed on an oxygen permeable slide (Permanox, Nalgen Nunc, 16005). Only samples with a few isolated axons were selected for subsequent live imaging. Image acquisition was performed on a Nikon Optiphot-2 microscope equipped with a 20× Plan NeoFluar objective and Orca-ER cooled CCD camera (Hammamatsu). To minimize phototoxicity, acquisitions were made with neutral density filters on and short exposure times (50–100 ms).

RESULTS & DISCUSSION

Having previously demonstrated the significant effect of TACC3 in promoting axon outgrowth, through increased number and length of axons, I sought to evaluate TACC3's effect on axon guidance. To study this, I obtained a grant to travel to the Holt lab at the University of Cambridge. The Holt lab has thoroughly characterized the guidance of retinal ganglion cells (RGCs) in developing *Xenopus* embryo brains, making their outgrowth an effective model of studying the ability of neurons to respond to guidance cues. They have also pioneered the development of a few powerful and specific means of manipulating, studying, and quantifying RGC guidance *in vivo.* At Cambridge I performed two classes of experiments on TACC3: first, to replicate the effects of TACC3 KD on RGCs themselves, and second to study the *in vivo* guidance of these neurons in the developing brain.

First, I had to evaluate the phenotypic effects of TACC3 knockdown on Retinal Ganglion Cell outgrowth. We had previously demonstrated TACC3's role in axon outgrowth in neural tube-derived neurons (Nwagbara *et al.,*2014). This population of neurons is totally heterogeneous, however, being comprised of the developing central nervous system of the entire body of the embryo. Neurons from the various sub-groups that comprise the spinal cord express and regulate genes in diverse ways, and may respond very differently to varying growing conditions and guidance cues, or even whole-embryo genetic manipulation. It was possible that, for some reason, the RGCs might be resistant to the phenotypic effects of TACC3 KD.

To demonstrate the effect of TACC3 knockdown on RGCs, I performed a number of TACC3 and Control morpholino (MO) injections, then allowed the embryos to develop to stages 30-32, then dissected out the primordial eyes and plated on laminin-coated coverslips similar to those used for neural tube explant experiments. The RGCs were allowed to grow out and were imaged 24 hours later. These data illustrate the same significant effect of TACC3 KD on RGC axon outgrowth as demonstrated in neural tube-derived neurons (Figure 12).

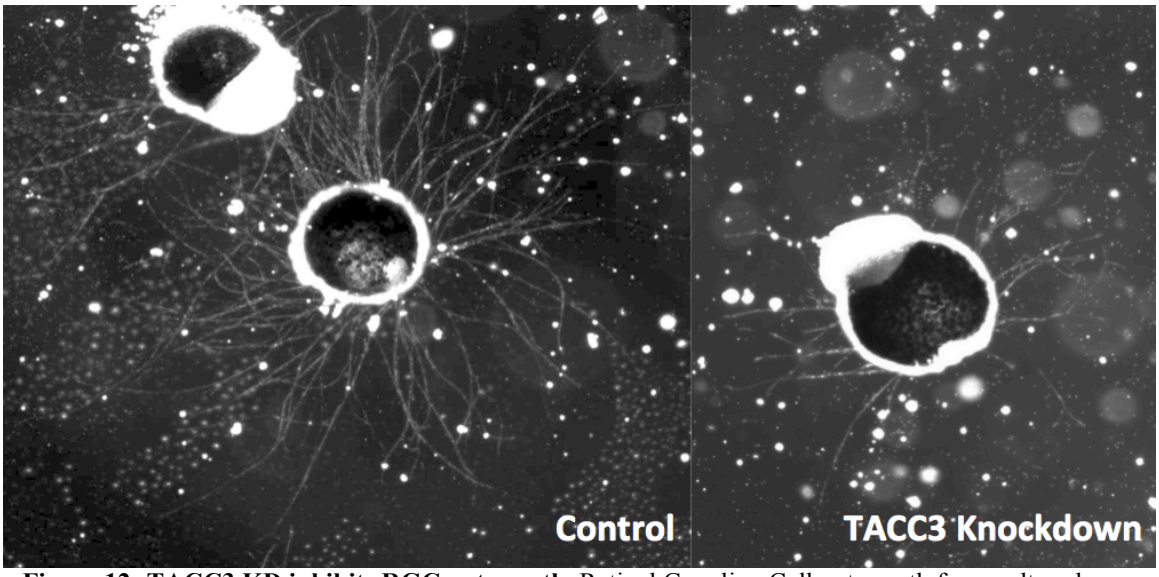

Figure 12: TACC3 KD inhibits RGC outgrowth. Retinal Ganglion Cell outgrowth from cultured stage 32 *Xenopus* embryonic eye explants, demonstrating significant reduction of axon outgrowth with TACC3 KD. Axon length was also significantly reduced, shown by the quantification plot of axon length below.

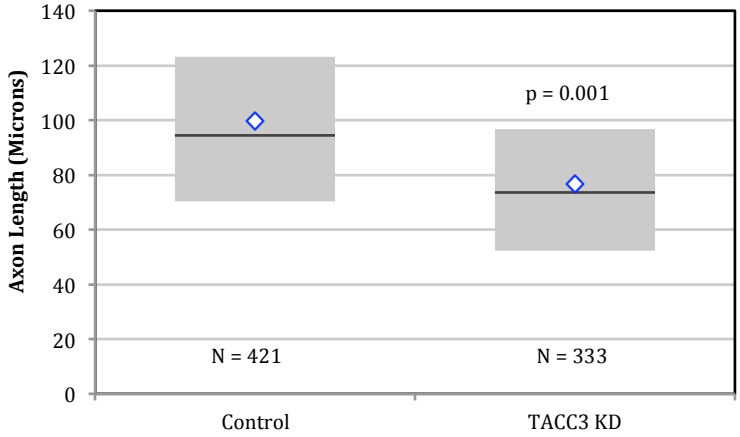

Following this demonstration of TACC3's phenotypic effect conservation between spinal neurons and RGCs, I then sought to examine the effect of TACC3 KD on RGC axon guidance *in vivo*. The retina of one eye of stage 30 *Xenopus* embryos was electroporated with membrane-targeted RFP. This enabled effective fluorescent labeling of the optic nerve (all RGC axons) in the developing brain. When imaged with the ventral prep technique described above, these experiments examined the effects of TACC3 knockdown on RGC guidance *in vivo* compared to control morpholino-injected embryos.

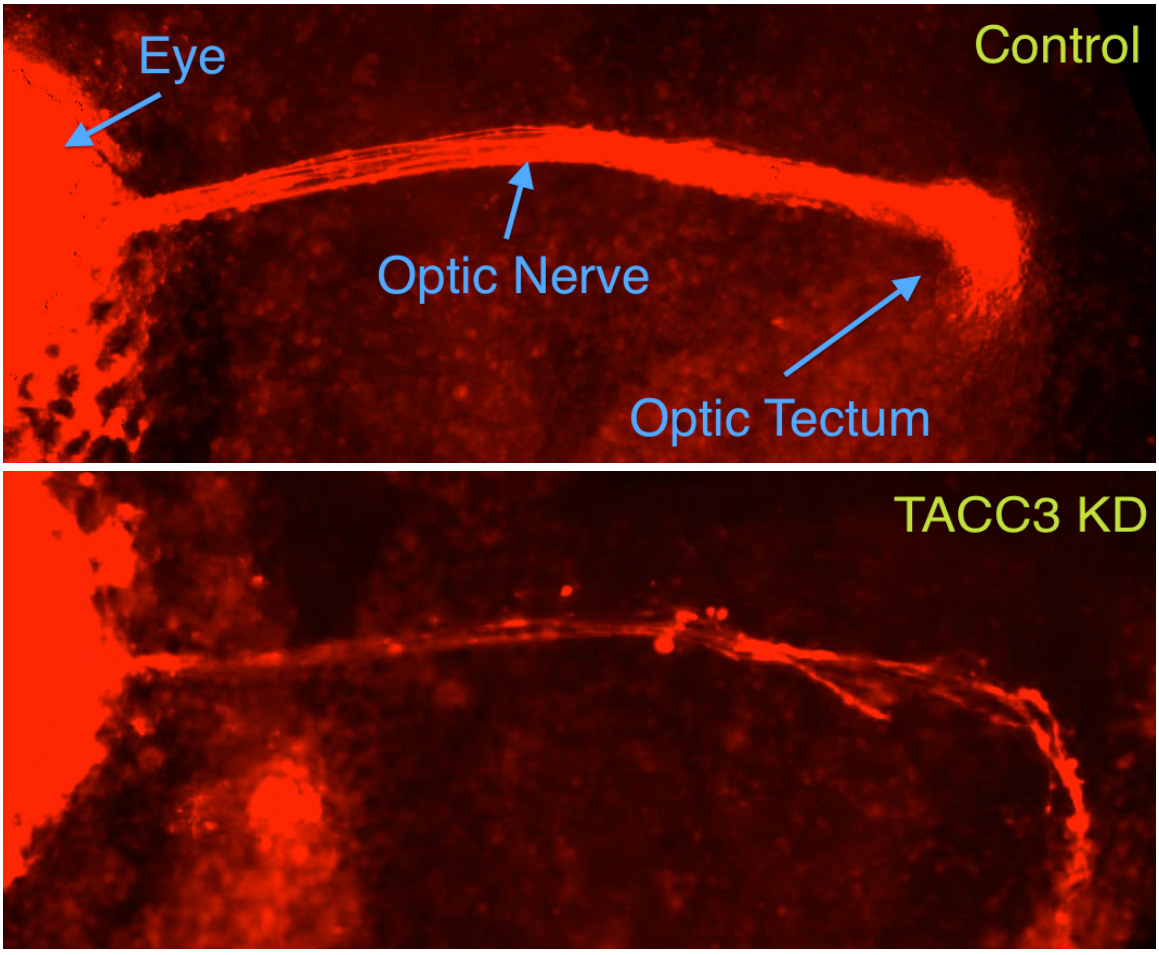

Figure 13: TACC3 affects RGC outgrowth and guidance *in vivo*. Compared to controls, TACC3 KD embryos demonstrated reduced outgrowth, sloppy fasciculation, and improper termination before or after reaching the optic tectum.

These results demonstrate a significant phenotypic discrepancy in axon guidance between embryos injected with TACC3 morpholino and the control (Figure 13). The axons comprising the optic nerve in the TACC3 KD embryos demonstrate sloppier fasciculation (the process by which growth cones follow existing axons), with some veering off the optic nerve track and terminating early. Some axons seem to migrate past the optic tectum area, missing their synaptic targets. Furthermore significantly fewer RGC axons even grew out from the electroporated eye in the first place. These data indicate TACC3 has an important role in axon guidance in the developing brain.

Taken together, these data collectively implicate TACC3 as a vital component of the process of neuron development. TACC3 promotes axon outgrowth and increased axon length, and appears to enable proper axon guidance. The mechanisms by which it does this probably involve regulation of its presence on the growing +end of dynamic microtubules in the growth cone periphery. Regulation of TACC3 on the +end may in turn regulate the behavior of its binding partner XMAP215, to regulate polymerization of these dynamic microtubules and build the scaffolds of growth cone migration.

Through these putative processes, TACC3 may well be a critically important effector protein of a number of growth factors and guidance cues. Through regulating the growth and polymerization of dynamic microtubules, TACC3 may be the final stage of translating these extracellular signals to an effect on the growth cone cytoskeleton. Signaling kinases or proteases may phosphorylate, dephosphorylate, or cleave the TACC3 protein to regulate its localization and binding partners, to produce this regulatory effect. To evaluate this hypothesis, I had to examine the structure of TACC3 and how it’s binding to microtubule +ends may be dynamically regulated.

Chapter III: The Structure and Function of TACC3

In order to understand how TACC3 affects axon outgrowth and guidance, it was necessary to understand the mechanisms by which it binds the +ends of dynamic microtubules in the growth cone, and how this binding is regulated. To do this I began an analysis of the structural features of TACC3, and how each affected its ability to track microtubule +ends in the growth cone. Our lab had obtained a DNA construct of the TACC3 gene product extracted from *Xenopus* embryos (Barnard *et al*., 2005) and I fully sequenced it to confirm the exact protein sequence of TACC3. Comparisons of the *Xenopus* TACC3 sequence to those of human and other vertebrates revealed a number of conserved domains worthy of analysis. I then proceeded to subclone a series of deletion constructs, each eliminating a series of residues pertaining to one or more of these domains, and compared the localization of the resulting constructs.

MATERIALS & METHODS

Xenopus Embryos

Eggs obtained from female *Xenopus laevis* frogs (NASCO, Fort Atkinson, WI) were fertilized in vitro, dejellied, and cultured at 13–22°C in 0.1X Marc's modified Ringer's (MMR) using standard methods (Sive *et al*., 2010). Embryos were staged according to Nieuwkoop and Faber (1994). All experiments were approved by the Boston College Institutional Animal Care and Use Committee and were performed according to national regulatory standards.

Culture of Xenopus embryonic neural tube explants

Embryos were cultured in 0.1× MMR at 22°C to stages 22–24, and each neural tube was dissected into approximately 20 similarly sized explants (Tanaka and Kirschner,

1991; Lowery *et al*., 2013). The neural tube explants were plated in culture medium on poly-l-lysine (100 µg/ml)– and laminin (20 µg/ml)-coated coverslips attached to a plastic culture dish with a hole drilled in the center (imaging chambers described in Gomez *et al*., 2003). Outgrowing axons and neural crest cells were imaged at room temperature 18–24 h after plating. For imaging of nonneural cells, somite tissue flanking the neural tube was dissected and plated on poly-l-lysine (100 µg/ml)– and fibronectin (100 µg/ml)-coated coverslips.

TACC3 Sequencing

The following primers were designed and used to sequence GFP-TACC3 in pCS2+ to derive its exact proteomic sequence. EtonBio sequencing services were used.

Oligo0161	5'-AAGCTGATCTTCCAAGCCTTAC-3'
Oligo0165	5'-AGCTTCAGAACTCACCAGCA-3'
Oligo0219	5'-TGAAGATCGAGCACACAAGCGGAAGATC-3'
Oligo0220	5'-GCAGCACCAGAATCCTGGG-3'
Oligo0223	5'-ACCATCACACAAATTCTAGAG-3'
Oligo0226	5'-GCCTTCAAACTCTGCAATTATTTTC-3'

Constructs and RNA

Capped mRNA was transcribed in vitro using SP6 or T7 mMessage mMachine Kit (Life Technologies, Grand Island, NY). RNA was purified with LiCl precipitation and resuspended in nuclease-free water. The following table lists DNA constructs used to make mRNA for experiments, and where the constructs came from:

GFP-TACC3 in pCS2+	TACC3 pET30a was gift from the Richter lab, University of Massachusetts Medical School, Worcester, MA. Subcloned into GFP pCS2+ expression vector.
GFP-TACC3-Ndel	Subcloned from GFP-TACC3
GFP-TACC3-CC2del	Subcloned from GFP-TACC3
GFP-TACC3-CC1/2	Subcloned from GFP-TACC3
GFP-TACC3-BigdelN	Subcloned from GFP-TACC3
GFP-TACC3 Middle	Subcloned from GFP-TACC3
GFP-TACC3 Δ771-774	Subcloned from GFP-TACC3
GFP-TACC3 Δ775-781	Subcloned from GFP-TACC3

TACC3-GFP	Subcloned from GFP-TACC3
mKate2-tubulin in pT7TS	(Shcherbo *et al*., 2009)
EB1-GFP in pCS107	A gift from the Danilchik lab, Oregon Health Sciences University, Portland, OR
mKate2-EB1 in pCS2+	Subcloned from EB1-GFP

The dorsal blastomeres of embryos were injected four times at the two- to four-cell stage (in 0.1× _MMR containing 5% Ficoll) with the following total mRNA amount per embryo: 100–300 pg of EB1-GFP or mKate2-EB1, 900 pg of mKate2-tubulin, and 1000-2000 pg of GFP-TACC3 and each derived mutant TACC3 construct.

Subcloning

TACC3 deletion constructs were subcloned from GFP-TACC3 in pCS2+ using a variety of NEB High Fidelity Restriction Enzymes, as well as Quick Ligase, Antarctic Phosphatase, and Blunting Enzymes. For the deletions Δ771-774 and Δ775-781, the NEB Q5 SDM kit was used. Constructs were transformed into Top 10 Competent Cells using normal transformation protocols.

Confocal Microscopy

Live images were collected with a Yokogawa CSU-X1M 5000 spinning disk confocal on a Zeiss Axio Observer inverted motorized microscope with a Zeiss 63X Plan Apo 1.4 numerical aperture (NA) lens. Images were acquired with a Hamamatsu OCRA R2 charge-coupled device camera controlled with Zen software (Zeiss, Thornwood, NY). For time lapse, images were collected every 2 s for 1-3 min. Laser power for 488 nm was 30%, with exposure time 1000-1500 ms. Laser power of 561 nm was 25%, with exposure time 850–1500 ms.

RESULTS & DISCUSSION

Based on my acquired sequencing data, I was able to determine which structural domains of Xenopus TACC3 were highly conserved with human TACC3, and therefore likely to be important to the function of TACC3 (Figure 14). The family of TACC proteins all contain two ~100 amino acid coiled-coil domains (Figure 14, blue and purple) on their C-terminal (Still et al., 2004). This domain is highly conserved between humans and *Xenopus*, with our TACC3 sequence being 63% identical and 80% homologous to the human TACC3 sequence (Accession no. Q9Y6A5). The beginning ~100 residues of the N-terminal of TACC3 (Figure 14, red) and a short phosphorylated

MSLQLINDENAGNDITAEKFDLLLNPQTTGRPSILRPSQKDNLPPK
PALKSTKVTFQTPMRDPQTLRIMTPSVANKPENVFLLEDCTQALE
QLHLSLPSSCGPNPVEINSVSNNQPDSEELPVRTTGAYSIDFDNFD
DINPFKSKTQMLNSPIKADLPSLTENIETTTPVVPADEASKQMVSLN
LSAANLDSPVTVQFSSESGYIGVSEKTALDDTLPLSESGIKDLQGL
NASSNNIEEPVPLDKDICSNNEKDDATMADSTCEGTSDAHTSSNNI
EEPVTLDKDICSSNEKDNAAVADSTCEGTSDAQSPLPIPKSSYSFD
PDQFDMMNPFKTGGSKLQNSPAGKKQTPPSADLNTAKTEPVKLE
FNFGDGDVSERKPPPKKLGKRPLLKTAAKKPSPKPEIASEKQEQQ
TAKPSEDEAIVPKASYKFDWEKFDDPNFNPFGCGGSKISSSPKGQ
KIANEQPSACTQGSKPEAECTASDMAPAENADEKDHGEIEPSQDS
GAAEDRSQAEDQSVALSKVEVPHEQTTDCSPVENETQPEVSLINE
EPSQKEVEHTSSDMTPPEINGTDSEFKLATEADFLLAADMDFKPA
SEIFSEGFRQPVEIDYLENFGTNSFKESVLRKQSLYLKFDPLLRESP
KKSAAGINLLPSVPLKCSSDLFGAIPEANFPLIPSIENEEKPKGLDLL
GTFTVADTALLIVDAPSSVAVPNPFLSTSDAIVEMLKYSQKDMDAAI
EAVRLEVQEKDLEVLEWKTKHEKLYLEYVEMGKIIAEFEGTITQILE
DSQRQKETAKLELNKVLQEKQQVQVDLNSMETSFSELFRLEKQKE
ALEGYRKNEEALKKCVEDYLVRIKKEEQRYQALKAHAEEKLNRAN
EEIAHVRSKAKSEATALQATLRKEQMKIQSLERSLEQKSKENDELT
KICDDLILKMEKI*

N-terminal
Conserved regulatory region
Repeat region
Coiled-coil 1 domain
Coiled-coil 2 domain
Conserved phosphorylated residues
eIF4E Binding Domain
XMAP Binding Domain?

Figure 14: TACC3 Sequence and Conserved Domains. Data acquired from alignment of sequenced *X. laevis* TACC3 with human, murine, and *X. tropicalis* TACC3. Phosphorylation sites found in Barnard *et al.,* 2005 and Kinoshita *et al.,* 2005.

region upstream of the coiled-coil domains (Figure 14, green) are also highly conserved. These domains became the primary focus of study when analyzing which regions of TACC3 are responsible for its various binding partners and localization activity. Additionally, TACC3 possesses a domain required for its interaction with eIF4E and regulation of translation (Figure 14, pink) (Barnard *et al*., 2005) and a significant

repeated region of 29 amino acids on the N-terminal half of the protein (Figure 14, orange).

In order to study the domains of interest of TACC3, and determine which were necessary for localization to the +end of microtubules, I began by subcloning a number of deletion constructs of N-terminal GFP-tagged TACC3 lacking certain specific domains of the protein (Figure 15).

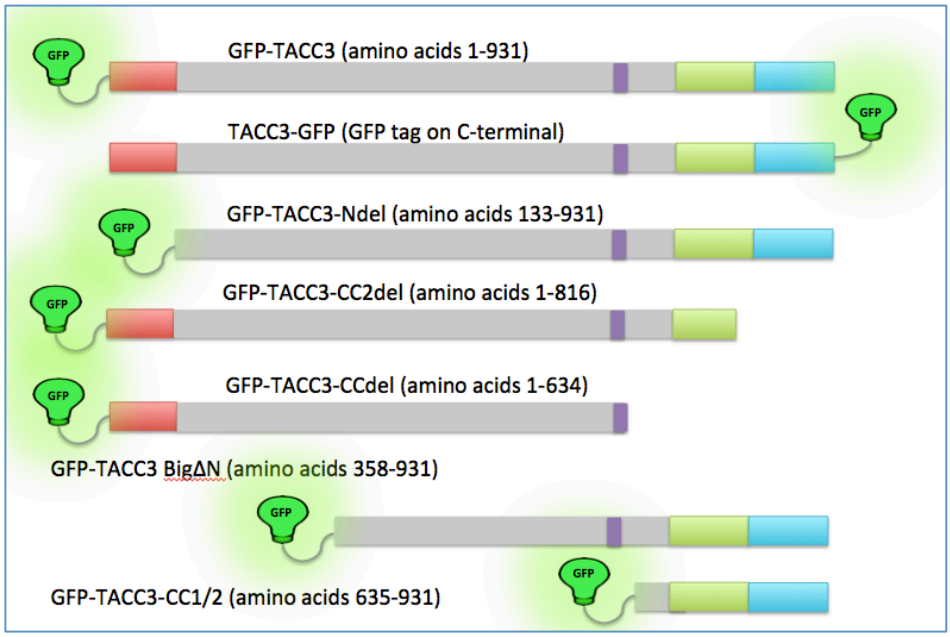

Figure 15: TACC3 Deletion Constructs subcloned from GFP-TACC3 (top), each isolating a different set of residues (shown in parentheses).

Each of these constructs was tested for +end-tracking localization in neural tube-derived growth cones, similar to the experiments used to first identify TACC3 as a +TIP in the first place. I made mRNA of each construct and co-injected it with mkate2-EB1 mRNA as a +TIP marker, and visualized the localization on a spinning disc confocal. The results indicated that the coiled-coil domains, and not the N-terminal, were necessary for TACC3 to +end-track in growth cones (Figure 16).

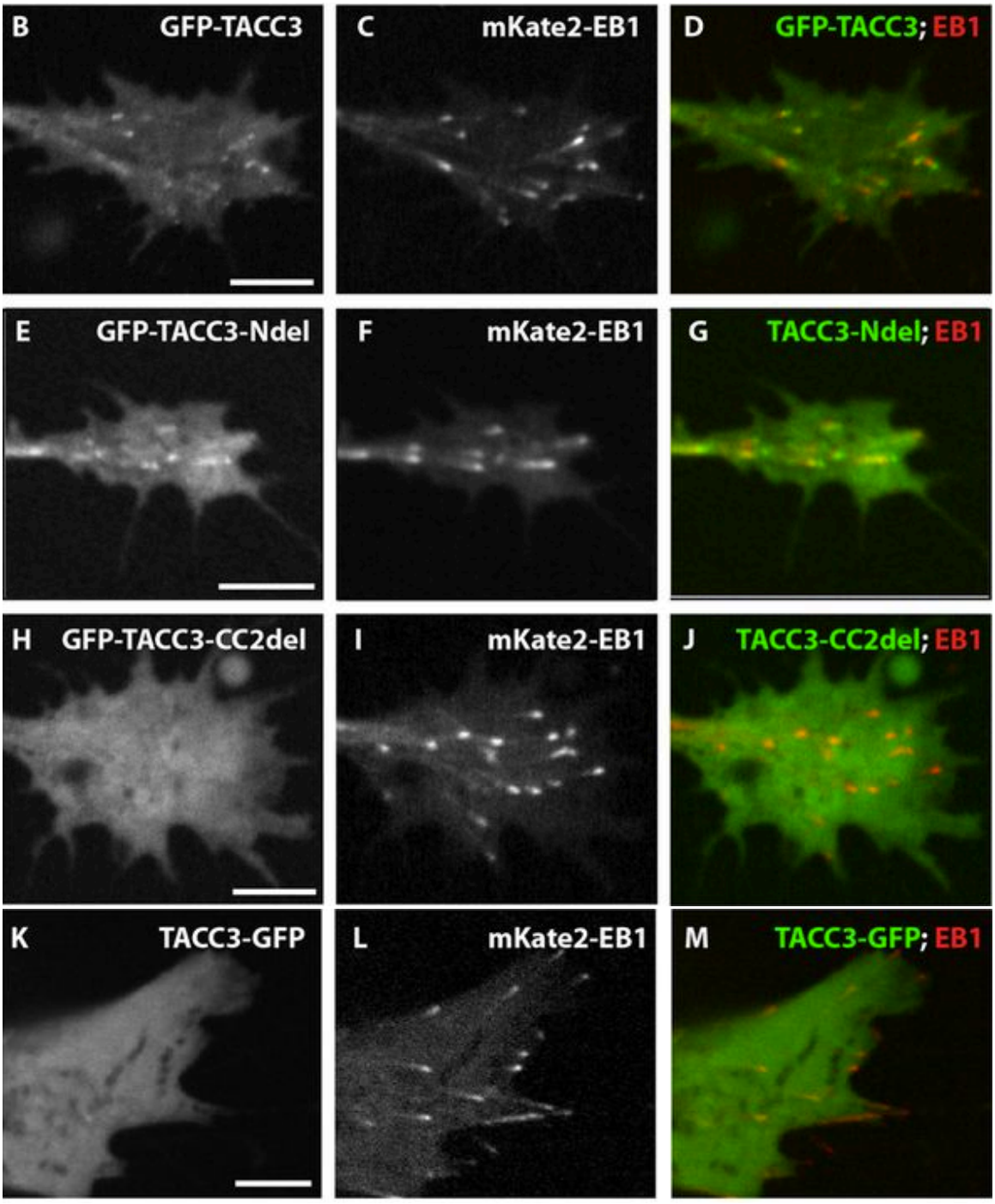

Figure 16: Green fluorescent constructs described in Figure 10 imaged alongside red fluorescent mkate2-EB1 as a +TIP marker. Bar = 5 µm. (Nwagbara et al., 2014, Figure 5 B-M).

Full length GFP-TACC3 was imaged alongside each construct as a control, and clearly tracks microtubule +ends in growth cones (Figure 16 B-D). When the conserved N-terminal region was deleted (GFP-TACC3-Ndel) TACC3 was still able to track

microtubule +ends (Figure 16 E-G). However, when the second coiled-coil domain was deleted (GFP-TACC3-CC2del) TACC3 was unable to +end track (Figure 16 H-J). These data indicated that TACC3's coiled-coils were what enabled its recruitment to the +TIP complex. This theory was further strengthened by the inability of TACC3-GFP (with GFP tagged to the C-terminal) to +end track (Figure 16 K-M), most likely due to steric hindrance of the coiled-coils by the adjacent GFP protein.

Having identified the C-terminal coiled-coil domains of TACC3 as the probable domain which mediates TACC3's +TIP activity, I then sought to isolate the coiled-coils themselves to see if they can still +end track independently. The construct GFP-TACC3-CC1/2 isolated both coiled-coils with a linker region on the N-terminal side linked to GFP, so as to avoid the steric hindrance issue seen with TACC3-GFP. However, this construct failed to +end track (Figure 17 bottom). Yet when we made another construct that isolated the C-terminal two-thirds of the protein, dubbed "TACC3 BigΔN", we found it *was* able to +end track (Figure 17 top).

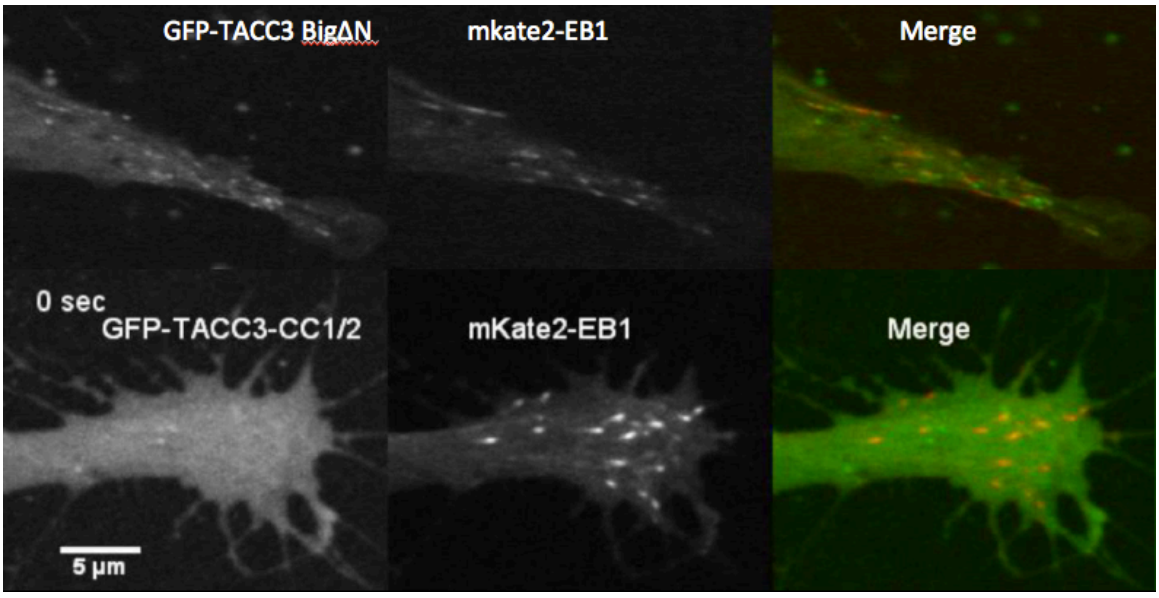

Figure 17: Green fluorescent constructs described in Figure 10 imaged alongside red fluorescent mkate2-EB1 as a +TIP marker.

These localization experiments demonstrate the necessity of more than just the coiled-coils of TACC3 to +end track. As the GFP-TACC3-CC1/2 construct also lacked the conserved phosphorylated domain implicated in the regulation of TACC3's behavior (Barnard *et al*., 2005), my focus has since turned to the role this domain may play in mediating TACC3's binding.

I also examined other studies that have focused on the means by which human TACC3 binds chTOG (XMAP215) to physically interact during mitosis, and narrowed down their binding domain to a short residue (Hood *et al*., 2013). This domain (Figure 14, light blue) consists of two sets of residues within the first coiled-coil domain, homologous to amino acids 771-774 "EFEG" and 775-781 "TITQILE" in *Xenopus*. Hood *et al.* 2013 demonstrated through X-ray crystallography that deleting one of these two regions did not disrupt the overall structure of the coiled-coils, despite each removing a significant section of the alpha helix. Although the *Xenopus* TACC3 protein sequence is slightly different, it is homologous enough (80%) to predict that these residues pertain to the same part of the coiled-coil, and deleting them should not significantly affect TACC3's coiled-coils, while effectively blocking TACC3's interaction with XMAP215.

I selectively deleted these residues, constructing two domains of full-length TACC3 lacking only one of these two short domains. These two constructs (GFP-TACC3 Δ771-774 and GFP-TACC3 Δ775-781) were both still able to +end track (Figure 18). These results indicate that these deletions did not disrupt the coiled-coil domain overall structure, as that would have blocked +end tracking ability entirely.

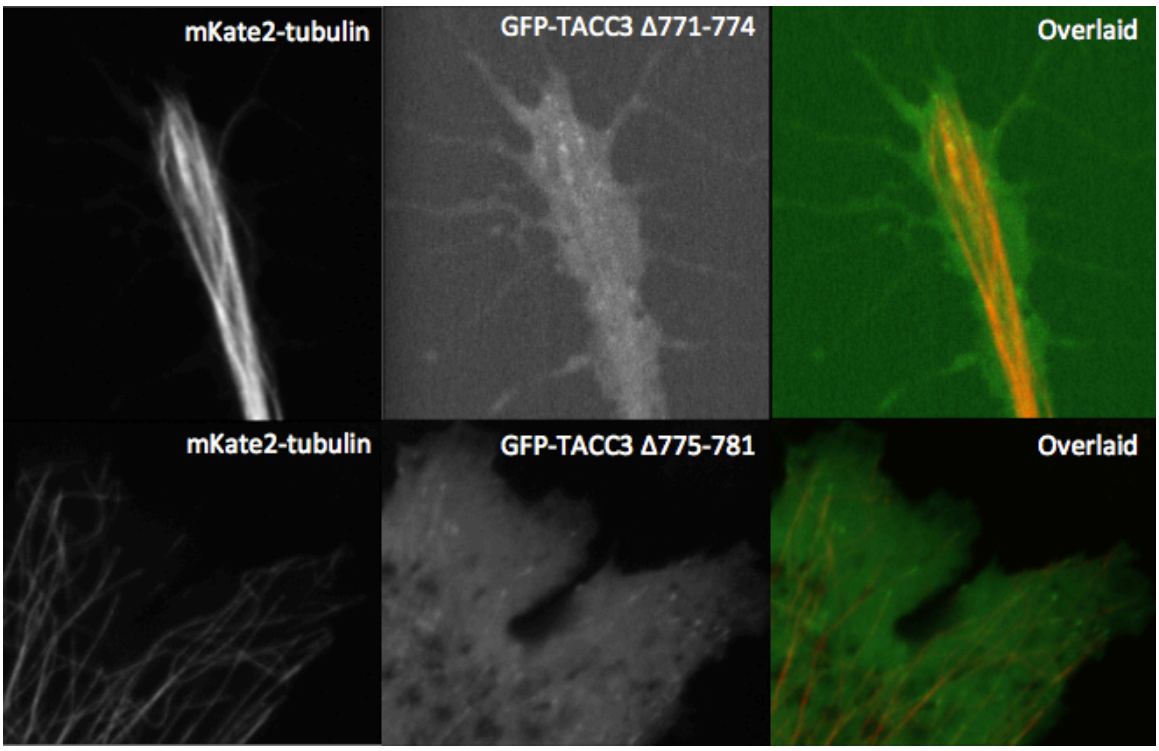

Figure 18: TACC3 constructs lacking suspected XMAP binding domain can still +end track. Green fluorescent TACC3 constructs selectively lacking the specified amino acid residues imaged alongside red fluorescent mkate2-tubulin to visualize microtubules. Top images are of a growth cone, bottom images are of a neural tube-derived mesenchymal cell.

This suggests that something besides TACC3's interaction with XMAP215 enables the coiled-coil domain to recruit TACC3 to the microtubule +end. This could be through binding and interacting with other +TIPs, or through a direct means of binding the polymerizing tubulin subunits. We are currently investigating the effects of TACC3 on the +end while unable to bind XMAP, as this may demonstrate a failure of these TACC3 deletion constructs when overexpressed to improve microtubule polymerization velocity and length, as wild-type TACC3 could (Figure 9).

I have determined that the coiled-coil domains are required for localizing TACC3 to growing microtubule +ends. However it is clear that more than just the coiled-coils is required for TACC3's recruitment. It is likely that the highly conserved and phosphorylated region just upstream of these domains mediates this recruitment, and this domain has become the focus of my latest series of projects. Understanding the

mechanisms of +end-binding of the coiled-coils and the structural regulation process behind them will help us elucidate the big picture of TACC3's role on the +end, most importantly *why* it is there in the first place, and what makes it bind there. This is essential to understanding the role of TACC3 in regulating dynamic microtubules in the growth cone, a key component of the cytoskeletal dynamics of neurodevelopment.

Chapter IV: TACC1

TACC3 was shown to play an important role in mediating axon outgrowth and guidance through its interaction with XMAP215 on the +ends of dynamic microtubules. It was demonstrated that this interaction was mediated through TACC3's coiled-coil domains. However TACC3 is not the only protein in vertebrates to possess these domains. The TACC protein family has three members in most vertebrates with published genomes: TACC1, TACC2, and TACC3. In humans, mice, and rats, the coiled-coil domains of these orthologous proteins is highly homologous, being almost 90% conserved. The coiled-coils of each TACC are also highly conserved between paralogs within each species' genomes, indicating a shared function.

Xenopus has been previously reported to only have TACC3 (Ha et al., 2013; Peset and Vernos, 2008). I searched the recently published *Xenopus* genomes on Xenbase and showed that both *X. laevis* and *X. tropicalis* have three TACC family members as well, although TACC1 and TACC2 were totally uncharacterized and only known from expressed sequence tag (EST data). Due to the high degree of conservation between the TACC family coiled-coils, and the demonstration that the coiled-coils of TACC3 are what mediates its +TIP behavior, I sought to examine the other TACC family members for similar, if not redundant, functions. Therefore I sought to clone *Xenopus laevis* TACC1 and TACC2 and study them in the same manner as TACC3.

MATERIALS & METHODS

Embryos

Eggs obtained from female *Xenopus laevis* frogs (NASCO, Fort Atkinson, WI) were fertilized *in vitro*, dejellied, and cultured at 13 – 22℃ in 0.1X Marc's modified

Ringer's (MMR) using standard methods (Sive *et al*., 2010). Embryos were staged according to Nieuwkoop and Faber (1994). All experiments were approved by the Boston College Institutional Animal Care and Use Committee (IACUC) and were performed according to national regulatory standards.

Culture of *Xenopus* Embryonic Explants

Embryos were cultured in 0.1X MMR at 22°C to stage 22-24, and embryonic explants were dissected and cultured on poly-L-lysine (100 µg /mL)- and laminin-coated (20 µg/mL) coverslips, as described previously (Lowery *et al*., 2012; Nwagbara *et al*., 2014). Cells were imaged at room temperature 18 - 24 hours after plating.

Constructs and RNA

Capped mRNA was transcribed *in vitro* using SP6 or T7 mMessage mMachine Kit (Life Technologies, Grand Island, NY). RNA was purified with LiCl precipitation and re-suspended in nuclease free water. Constructs used: GFP-TACC1, GFP-TACC1-Cterm, GFP-TACC1-Nterm (subcloned from GFP-TACC1), mKate2-tubulin (Shcherbo et al., 2009) in pT7TS, and mKate2-EB1 in pCS2+. The dorsal blastomeres of embryos were injected four times at the two-to-four cell stage (in 0.1X MMR containing 5% Ficoll) with total mRNA amount per embryo: 1000 to 2000 pg GFP-TACC1 and derived constructs, 100 to 300 pg EB1-GFP or mKate2-EB1, 900 pg mKate2-tubulin.

RT-PCR Time Course and Cloning of TACC1

Total RNA was extracted from staged wild-type embryos using Trizol reagent (Life Technologies, Grand Island, NY), followed by chloroform extraction and isopropanol precipitation. Total RNA was further purified with a phenol:chloroform extraction and an ethanol precipitation. cDNA synthesis was performed with Super Script

II Reverse Transcriptase (Life Technologies, Grand Island, NY) and random hexamers. PCR was then performed, with the following primers.

For cloning TACC1:

Forward: 5'-TTTTCTCGAGATGTCGTTCAGCCCGTGG-3'
Reverse: 5'-TTTTCTCGAGTCACTGCGTCCCATCTTTGC-3'

For testing the expression levels of TACC1, TACC3, and actin as a control:

TACC1 Forward: 5'-CTCGAGGGCTCATCACTCGAACTGGATG-3',
TACC1 Reverse: 5'-TTTTCTCGAGTCACTGCGTCCCATCTTTGC-3'
TACC3 Forward (Oligo 0165): 5'-AGCTTCAGAACTCACCAGCA-3'
TACC3 Reverse (Oligo 0220): 5'-GCAGCACCAGAATCCTGGG-3'
Actin Forward: 5'-AAGGAGACAGTCTGTGTGCGTCCA-3'
Actin Reverse: 5'-CAACATGATTTCTGCAAGAGCTCC-3'

For TACC1 cloning, the above primers were designed based upon the TACC1 annotated sequence from the *laevis* genome v6.0 gene model (www.xenbase.org). Specifically, we used the UTexas Oktoberfest transcript model of Scaffold27535:373746..413683, which was predicted to contain the *Xenopus laevis* TACC1 genomic sequence. The TACC1 mRNA sequence was submitted to Genbank, accession number KP866215.

Confocal Microscopy

Live images were collected with a Yokogawa CSU-X1M 5000 spinning disk confocal on a Zeiss Axio Observer inverted motorized microscope with a Zeiss 63X Plan Apo 1.4 numerical aperture (NA) lens. Images were acquired with a Hamamatsu OCRA R2 charge-coupled device camera controlled with Zen software (Zeiss, Thornwood, NY). For time lapse, images were collected every 2 s for 1-3 min. Laser power for 488 nm was 30%, with exposure time 1000-1500 ms. Laser power of 561 nm was 25%, with exposure time 850–1500 ms.

RESULTS & DISCUSSION

I designed primers and attempted to PCR these genes out of extracted *Xenopus* embryonic cDNA. Unfortunately this PCR was unsuccessful, but my colleague Chris was able to PCR TACC1 out of the cDNA later on, and we proceeded with a full analysis of TACC1's behavior.

After extracting the expressed sequence of the TACC1 gene, we sequenced it and compared it to *Xenopus* TACC3. This alignment demonstrated that the coiled-coils of the *Xenopus* TACC1 and TACC3 paralogs are highly conserved between each other (Figure 19), showing over 90% homology. This further warranted an analysis of the possibility that these proteins have similar functions. It also demonstrated that the highly conserved phosphorylated domain of TACC3 is notably absent in TACC1, indicating that while the coiled-coils may mediate similar localizations and functions, the regulation of the TACC

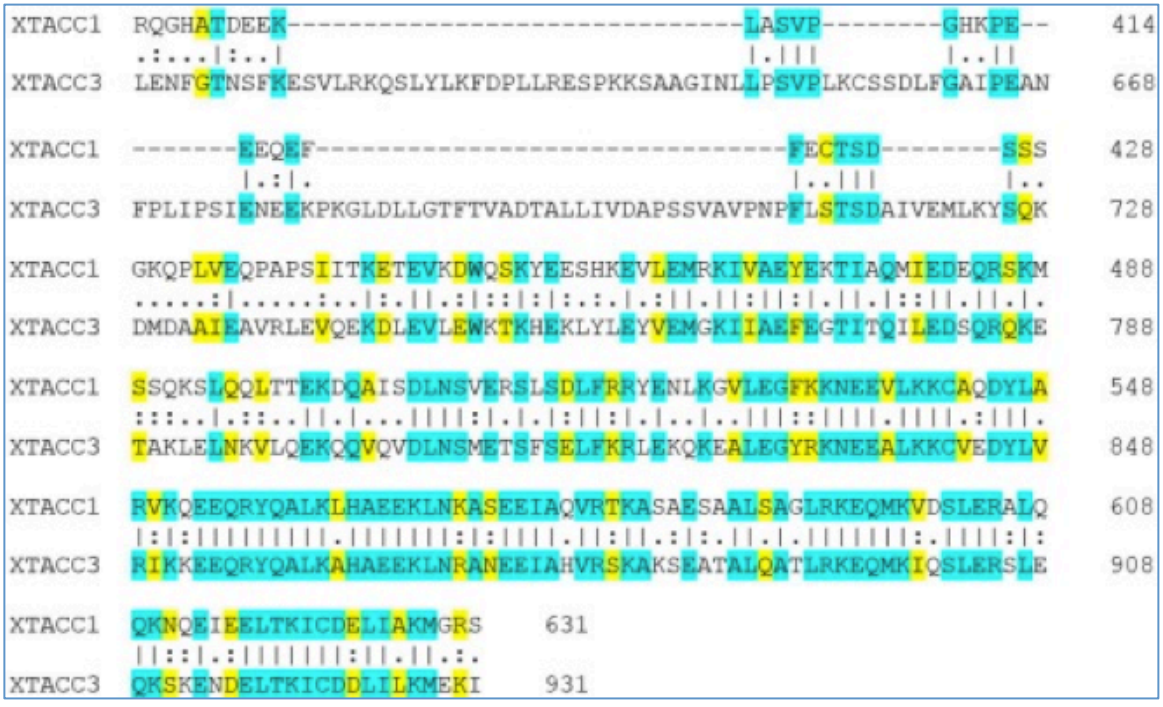

Figure 19: *X. laevis* TACC1 (top) and TACC3 (bottom) C-terminal alignment. The coiled-coils of TACC3 (a.a.s 744 – 931) are highly conserved in TACC1. The conserved phosphorylated region of TACC3 (a.a.s 619-641) are notably absent in TACC1.

family binding is likely to be rather different between paralogs.

Following the demonstration that TACC1 is present in *Xenopus* embryos and shares very similar coiled-coil domains, we needed to determine how TACC1 is expressed. It was possible that it is barely expressed at all, and that TACC3 has taken over many of the (possibly redundant) functions of TACC1. I performed RT-PCR expression analysis of TACC1, TACC3, and actin as a control for total gene expression levels (as actin mRNA levels remain relatively constant between cell types and stages). I compared expression levels in cDNA extracted from the blastula stage, about 6 hours post-fertilization, or stage 8 of *Xenopus* development (Nieuwkoop and Faber, 1994) to the neurula stage (1 day post-fertilization or stage 22) and early tadpole stages (2 days post-fertilization or stages 32-34). I also compared expression levels in epidermal, mesenchymal, and neural tissue.

These results (Figure 20) demonstrate that both TACC1 and TACC3 are highly expressed in early-stage embryos, probably due to a shared role in mitotic spindle assembly, far more important when the embryo is simply a ball of rapidly dividing cells.

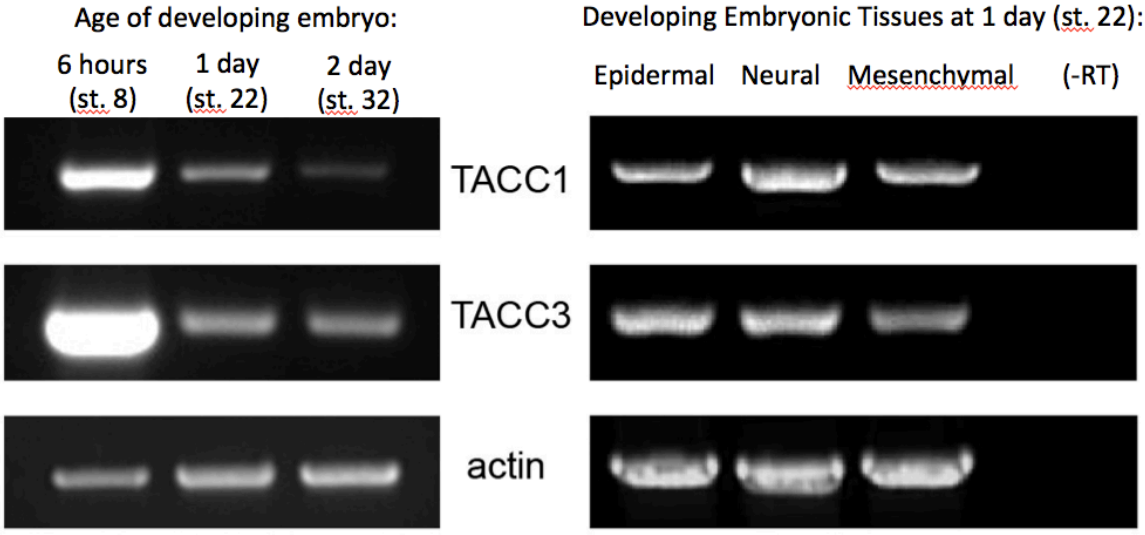

Figure 20: *Xenopus* TACC1 and TACC3 early expression levels. TACC1 and TACC3 expression levels are compared using quantitative PCR between 6 hours (blastula) 1 day (neurula) and 2 day (tadpole) post-fertilization developmental stages. Levels were also compared between epidermis, neural tube, and mesenchymal tissue. Actin used as a control for relative levels of total cDNA. (-RT) shows the same PCR done on extracted mRNA untreated with reverse transcriptase, as a control for contamination with genomic DNA.

The relative expression levels also showed that TACC3 remains expressed relatively constantly throughout the neurulation developmental process (about 1 day old, or stage 22) and early tadpole stages (about 2 days old, or stage 32). Unlike TACC3, however, TACC1 levels decline significantly following neurulation. TACC1 and TACC3 are both enriched in stage 22 nervous system tissue, although TACC1 appears proportionally more enriched. TACC1 remains present and expressed in neural tissue, and although its levels are not as significant as TACC3 when compared to earlier stages, it is still present and therefore worthy of behavioral examination.

Due to the high degree of homology in the coiled-coils, we predicted that TACC1 might have similar localization abilities as TACC3. We subcloned a construct of TACC1 into the GFP pCS2+ expression vector used for TACC3, and prepared mRNA of this construct to use for localization studies. Our localization studies demonstrate that TACC1 can indeed +end-track growing microtubules (Figure 21). This conservation of

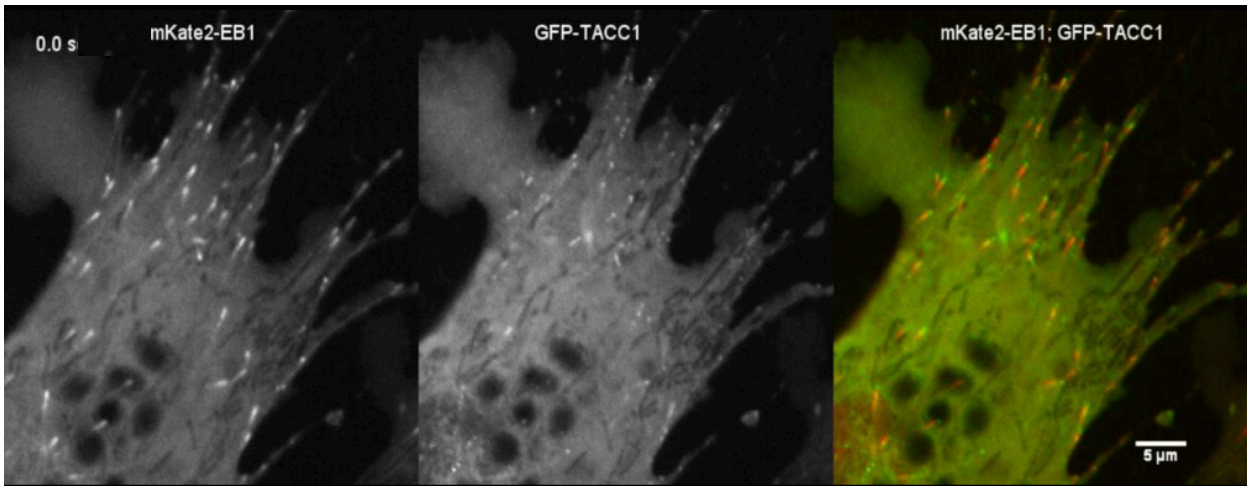

Figure 21: TACC1 is a +TIP. Fluorescent time-lapse imaging of GFP-TACC1 alongside mkate2-EB1 as a +TIP marker shows TACC1 clearly +TIP tracking in neural tube-derived mesenchymal cells. Bar = 5 µm.

localization indicates a shared function of the TACC family of proteins within the +TIP complex. Our lab's further experiments have shown this effect is maintained in neuronal growth cones as well as neural tube-derived mesenchymal cells and fibroblasts.

To determine if the coiled-coils were responsible for this interaction, we subcloned two constructs. One, GFP-TACC1-Nterminal, consisted of amino acids 1-370 of the TACC1 protein tagged with GFP. The other consisted of the remaining amino acids, 371-631. These constructs were co-injected with mkate2-EB1 to determine which, if either could localize to the +end of microtubules like the full TACC1 protein. We determined that like TACC3, TACC1 requires the C-terminal coiled-coil domains to localize to the +end (Figure 22). TACC1 C-terminal could still +end track just fine (Figure 22, top), whereas TACC1 N-terminal could not (Figure 22, bottom). These

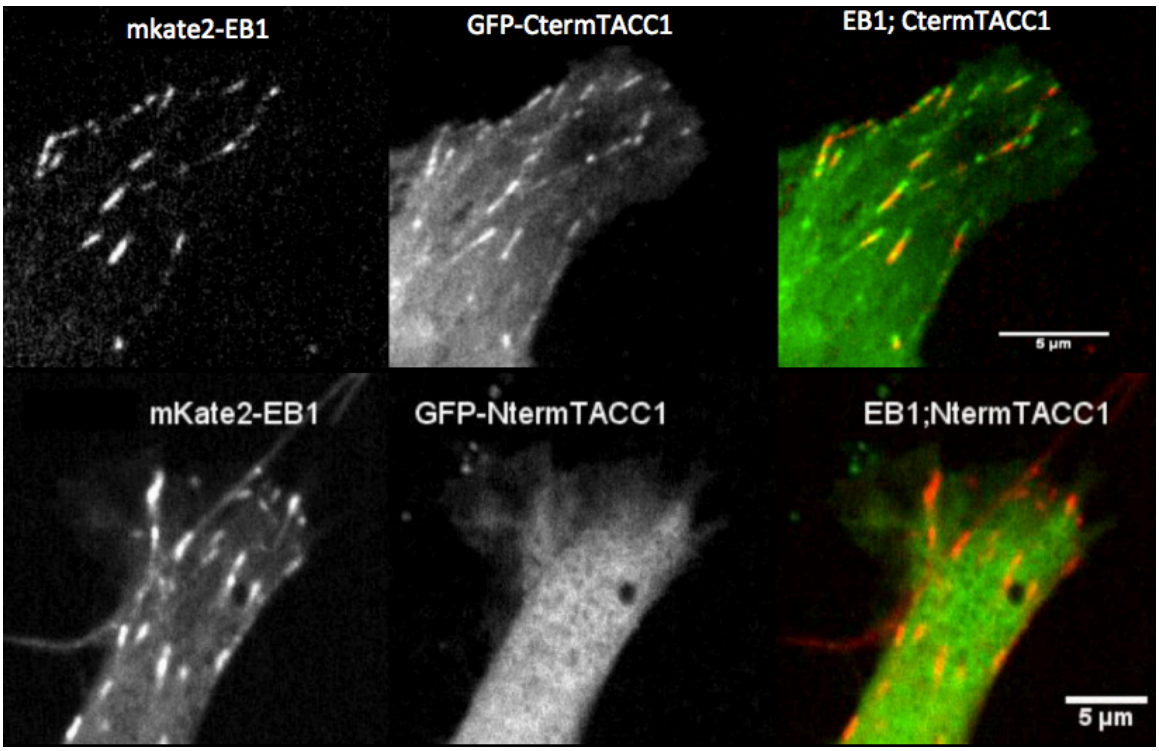

Figure 22: TACC1 requires its C-terminal to +end track. Fluorescent imaging of GFP-TACC1-Cterminal (a.a.s 371-631) on top and GFP-TACC1-Nterminal (a.a.s 1-370) on bottom, alongside mkate2-EB1 as a +TIP marker. TACC1 C-terminal shows a clear ability to +end track, unlike TACC1 N-terminal. Bar = 5 µm.

localization studies indicate a conservation of the role of the coiled-coils between TACC1 and TACC3. These structures are over 90% homologous between the paralogs, and are necessary to mediate the recruitment of both proteins to the +TIP complex of microtubules.

To determine if TACC1 shares similar functions as TACC3 on the +end of microtubules, our lab performed a number of additional TACC1 overexpression experiments to quantify TACC1's role in regulating microtubule dynamics. These data (submitted for publication as Lucaj and Evans *et al.,* 2015) demonstrated that TACC1 does have an effect in promoting microtubule polymerization (Figure 23) through increasing the polymerization velocity and total growth length of microtubules, but not the lifetime of microtubule growth. This profile is identical to that of TACC3's effect on microtubule dynamics, and indeed joint overexpression studies revealed that this effect is

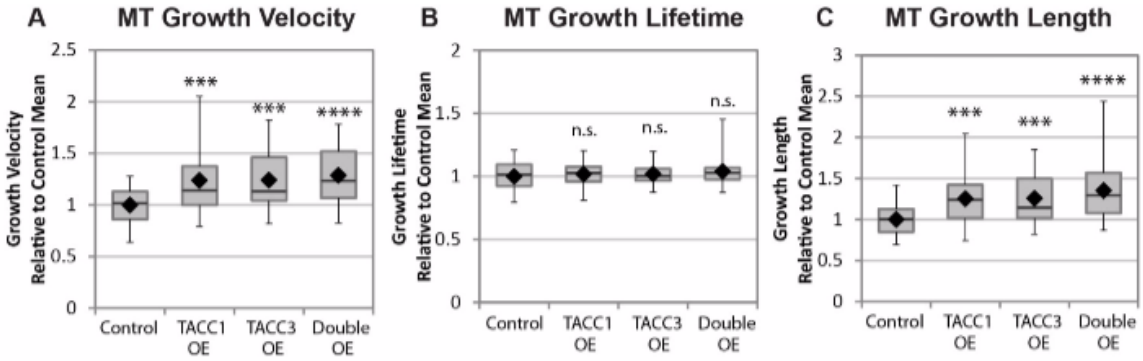

Figure 23: TACC1 promotes microtubule growth velocity and length, but not lifetime. Quantification of microtubule (MT) growth track parameters in cultured cells following overexpression (OE) of TACC1, TACC3, or both (double). EB1-GFP localizes to the ends of growing MTs and is thus a marker for MT polymerization. Automated tracking of EB1-GFP comets calculate MT growth-track velocity (A), MT growth-track lifetime (B), and MT growth-track length (C). An unpaired t test was performed to assess significance of over-expression conditions compared to control. ***$p<0.001$, ****$p<0.0001$; n.s., not significant.

synergistic; that increased levels of both TACC1 and TACC3 increase microtubule growth velocity and length more than either does independently.

The conservation of structure and function between the TACC family members indicates that this protein family may share the roles of TACC3 in neurodevelopment. The coiled-coil domains of each family member may serve to promote microtubule polymerization through interacting with XMAP215. The highly variable remainder of the protein may serve other functions, like those demonstrated for TACC3 in mitosis and translational regulation (Kinoshita *et al.,* 2005 and Barnard *et al.,* 2005), and for regulating the binding and activity of the coiled-coil domains within the +TIP complex. The differential regulation of TACC1 and TACC3 might serve as a mechanism by which different guidance cues or signaling cascades are translated into an effect on microtubule dynamics. Understanding the regulation of the TACC family members and how it affects localization to microtubule +ends is essential to elucidating how they may translate environmental signals to dynamic growth cone microtubules to enable correct guidance of developing neurons.

Chapter V: Future Directions

Regulation of the TACC Family

Our quest into the structure and function of the TACC family is only just beginning. This thesis and our recent publications have demonstrated that both TACC1 and TACC3 play an important role in regulating microtubule dynamics through their localization to the +TIP complex, mediated by their coiled-coil domains. Furthermore, I showed TACC3 to have an effect in mediating axon guidance *in vivo*. Based on these data and the nature of +TIPs in regulating dynamic microtubules in growth cones, I believe that TACC3 (and possibly the other TACCs) are the target of signaling cascades begun on the growth cone membrane by guidance cues. The central role of the TACC family in neurodevelopment may to translate these signals into an effect on the growth cone cytoskeleton, promoting microtubule growth towards positive guidance cues or away from negative guidance cues.

In order to confirm or refute this hypothesis, we must first fully understand exactly how the +end-binding activity of the TACCs is regulated in the first place. There are a number of means by which TACC3 and the other TACCs might be regulated, including (but not limited to) alternative splicing, proteolytic cleavage, and phosphorylation by signaling kinases. I have begun to study the regulation of TACC3 by each of these processes, although unfortunately my time in the Lowery Lab is limited and I will not be able to complete this analysis. The frameworks of these future experiments are presented here.

We determined that TACC3 is alternatively spliced in nervous system tissue, compared to the gene expressed in earlier-stage *Xenopus* embryos. We PCR'ed TACC3 out of cDNA extracted from isolated axons, and I used the same primers used to fully sequence our original TACC3 (See Chapter III Materials & Methods) to sequence neural TACC3 and compare any discrepancies. I determined that a significant portion of the

mid-section double repeat domain of TACC3 is alternatively spliced out of the TACC3 mRNA present in neurons (Figure 24). This alignment demonstrated that this double repeated section must be relevant in some way to the functional differences between

```
1    MSLQLINDENAGNDITAEKFDLLLNPQTTGRPSILRPSQKDNLPPKPALKSTKVTFQTPM  60
     MSLQLINDENAGNDITAEK DLL +P TTGRPSILRPSQK NLPPKP LKS KVTFQTPM
1    MSLQLINDENAGNDITAEKCDLLFSPPTTGRPSILRPSQKVNLPPKPTLKSIKVTFQTPM  60

61   RDPQTLRIMTPSVANKPENVFLLEDCTQALEQLHLSLPSSCGPNPVEINS-VSNNQPDSE  119
     RDPQT RIMTPSVANKP N FLLEDCTQALEQLHLS+PS+CGPNPVE N  VS NQPDS+
61   RDPQTQRIMTPSVANKPANAFLLEDCTQALEQLHLSVPSNCGPNPVETNKLVSANQPDSD  120

120  ELPVRTTGAYSIDFDNFDDINPFKSKTQMLNSPIKADLPSLTENIETTTPVVPADEASKQ  179
     ELP+ +TGAYSIDFDN DD+NPFKSKTQMLNSPIKADLPS  EN+E TTPV+PA EASK
121  ELPMSSTGAYSIDFDNLDDLNPFKSKTQMLNSPIKADLPSHMENMEATTPVIPAGEASKH  180

180  MVSLNLSAANLDSPVTVQFSSESGYIGVSEKTALDDTLPLSESGIKDLQGLNASSNNIEE  239
     M S N SAANLDSPVTVQFSSES  +GVS+K ALDDTLPLSESGIKDLQG N SSN+IEE
181  MESSNTSAANLDSPVTVQFSSESNTVGVSDKYALDDTLPLSESGIKDLQGSNKSSNSIEE  240

240  PVPLDKDICSNNEKDDATMADSTCEGTSDAHTSSNNIEEPVTLDKDICSSNEKDNAAVAD  299
     PV LDKD+CS+NEK                      N+E                  AV D
241  PVSLDKDMCSSNEK--------------------NVE------------------AVTD  261

300  STCEGTSDAQSPLPIPKSSYSFDPDQFDMMNPFKTGGSKLQNSPAGKKQTPPSADLNTAK  359
        E  SDAQSP P+PKSSYSFD D  DM+NPFKTGGSKLQNSPAG KQTPP  D+N AK
262  ---EANSDAQSPPPVPKSSYSFDLDHIDMINPFKTGGSKLQNSPAGVKQTPPPEDVNVAK  318

360  TEPVKLEFNFGDGDVSERKPPPKKLGKRPLLKTAAKKPSPKPEIASEKQEQQTAKPSEDE  419
     TEPVKLEFNF DGD   RKPPPKKLGKRP +KTA KKP PK E  +EKQE QTAKP EDE
319  TEPVKLEFNFSDGDAPARKPPPKKLGKRPPVKTATKKPVPKQETTAEKQETQTAKPVEDE  378

420  AIVPKASYKFDWEKFDDPNFNPFGCGGSKISSSPKGQKIANEQPSACTQGSKPEAECTAS  479
      +VPKASY+FDWEKFDDPNFNPFGCGGSK+SSSPKGQK+ANE  +AC    KP+AE T
379  VVVPKASYEFDWEKFDDPNFNPFGCGGSKVSSSPKGQKVANEVQAAC----KPKAEDT--  432

480  DMAPAENAD-EKDHGEIEPSQDSGAAEDRSQAEDQSVALSKVEVPHEQTTDCSPVENETQ  538
     D+ PAENAD +KD GEIEP+QDSG AED+S  EDQ V LS  ++PHEQTT+ SPVENETQ
433  DLTPAENADGKKDLGEIEPAQDSGVAEDKSHTEDQPVVLSNADLPHEQTTESSPVENETQ  492

539  PEVSLINEEPSQKEVEHTSSDMTPPEINGTDSEFKLATEADFLLAADMDFKPASEIFSEG  598
     PE+  + +EP QKEV+H S D+TPPEINGTDSEFKLATEADFL AADMDFKPASEIFSEG
493  PEICTVRDEPFQKEVDHRSPDITPPEINGTDSEFKLATEADFLPAADMDFKPASEIFSEG  552

599  FRQPVEIDYLENFGTNSFKESVLRKQSLYLKFDPLLRESPKKSAAGINLLPSVPLKCSSD  658
     F  P+EIDYLENFG+NSFKES LRKQSLYLKFDPLLRESPKK+AAG +LLPSVPLK S +
553  FGHPIEIDYLENFGSNSFKESALRKQSLYLKFDPLLRESPKKNAAGNSLLPSVPLKSSFE  612

659  LFGAIPEANFPLIPSIENEEKPKGLDLLGTFTVADTALLIVDAPSSVAVPNPFLSTSDAI  718
     LFG I E NFPLIPS ENEEKPKGLDLLGTFTVAD A LIVDAPSSVAVP+PFL TSDAI
613  LFGGISEVNFPLIPSFENEEKPKGLDLLGTFTVADAAPLIVDAPSSVAVPDPFLLTSDAI  672

719  VEMLKYSQKDMDAAIEAVRLEVQEKDLEVLEWKTKHEKLYLEYVEMGKIIAEFEGTITQI  778
     VE+LKYSQKDMDAAIEAVRLEVQEKDLEVLEWK +HEKLYLEYVEMGKIIAEFEGTITQ+
673  VEVLKYSQKDMDAAIEAVRLEVQEKDLEVLEWKNRHEKLYLEYVEMGKIIAEFEGTITQM  732

779  LEDSQRQKETAKLELNKVLQEKQQVQVDLNSMETSFSELF-RLEKQKEALEGYRKNEEAL  837
     LEDSQRQKE +KLE+NKVLQEKQQVQVDLNSME SFSELF RLEKQKE LEGYRKNEEAL
733  LEDSQRQKEMSKLEINKVLQEKQQVQVDLNSMEKSFSELFKRLEKQKEVLEGYRKNEEAL  792

838  KKCVEDYLVRIKKEEQRYQALKAHAEEKLNRANEEIAHVRSKAKSEATALQATLRKEQMK  897
     KKCVEDYL RIKKEEQRYQALKAHAEEKL+RANEEIAHVRSKAK+E+TALQATLRKEQMK
793  KKCVEDYLARIKKEEQRYQALKAHAEEKLSRANEEIAHVRSKAKAESTALQATLRKEQMK  852

898  IQSLERSLEQKSKENDELTKICDDLILKMEKI  929
      QSLERSLEQKSKENDELTKICDDLILKMEKI
853  TQSLERSLEQKSKENDELTKICDDLILKMEKI  884
```

Figure 24: Alignment of Neural TACC3 and Full-Length (Blastula) TACC3 Spliceoforms. Full-length TACC3 (top) was aligned with fully sequenced neural TACC3 (bottom), demonstrating five small splicing differences between amino acids 245 and 479 (of full TACC3).

neural TACC3 and the full-length TACC3 present in early-stage blastula embryos. The high degree of single nucleotide polymorphisms are likely due to high variability found within *Xenopus laevis* genomes.

The spliced-out region in neural TACC3 was shown to be unnecessary for TACC3's +end-binding abilities, however, as the "TACC3 BigΔN" construct was still able to +TIP track (Figure 17). As the other discrepancies in amino acid sequence are minor enough and the coiled-coil domains in neural TACC3 are still present, we know that neural and full TACC3 both +end-track via the same mechanisms. However, the fact that this exact double repeat section was mostly spliced out in neural TACC3, as well as a few other residues, indicates that some

functional difference between the spliceoforms may be relevant in the behavior of neural TACC3, and therefore these regions warrant further investigation.

In addition to determining that TACC3 is alternatively spliced in neurons, we sought to investigate if TACC3 is proteolytically cleaved. We performed a Western blot of embryos injected with mRNA of either GFP-TACC3 or TACC3-GFP (N- or C-terminal tagged, respectively) and blotted with a GFP antibody or a TACC3 antibody targeting the coiled-coil domains. These results demonstrated that TACC3 is indeed proteolytically cleaved *in vivo*, and that each (known) cleavage product appears to include the coiled-coil domains (Figure 25).

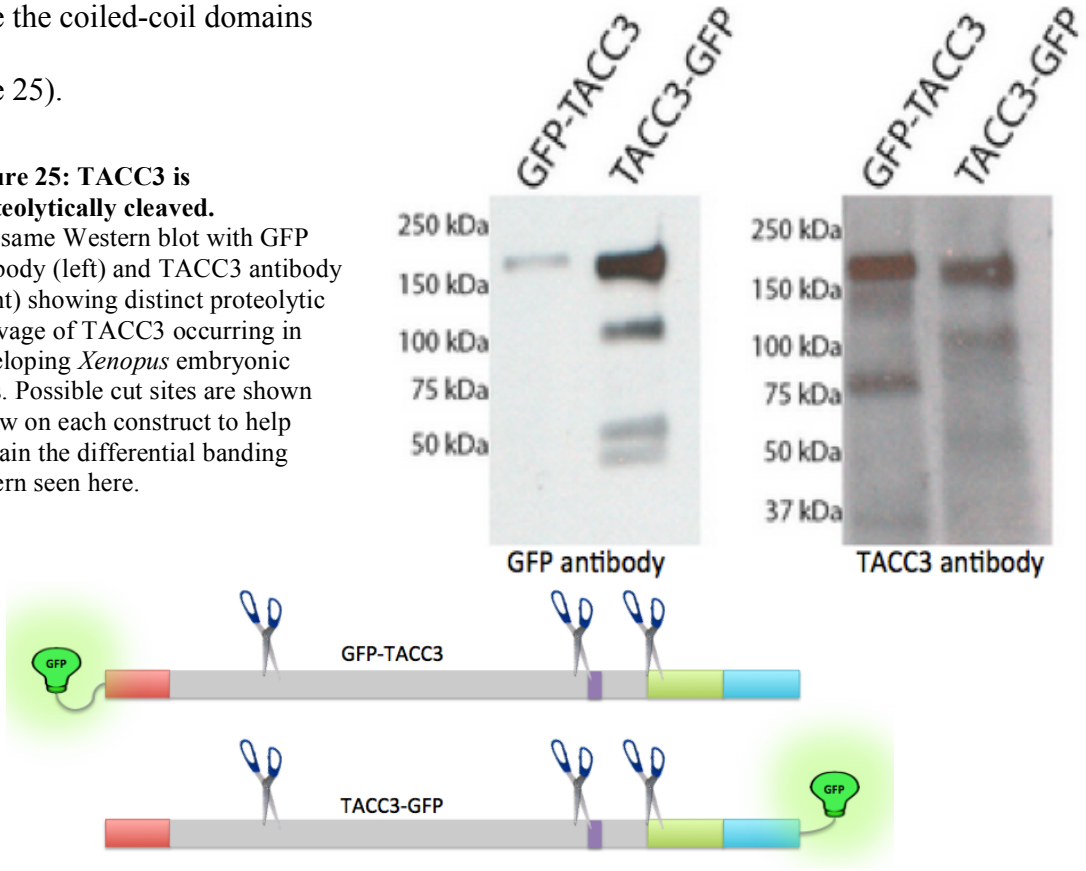

Figure 25: TACC3 is proteolytically cleaved. The same Western blot with GFP antibody (left) and TACC3 antibody (right) showing distinct proteolytic cleavage of TACC3 occurring in developing *Xenopus* embryonic cells. Possible cut sites are shown below on each construct to help explain the differential banding pattern seen here.

These data demonstrate that proteolytic cleavage of TACC3 does occur *in vivo*. The largest band corresponds to the full-length isoform of TACC3, the only one that can be detected by a GFP antibody in embryos injected with GFP-TACC3. However, in

embryos injected with TACC3-GFP, four distinct molecular weights can be detected; full-length TACC3 and three smaller isoforms, indicating TACC3 is proteolytically cleaved at three sites, each removing the N-terminal side of the protein for degradation. Possible cut sites are shown at the bottom of the figure. The bands detected in the GFP-TACC3 lane by the TACC3 antibody correspond to the remainder of the cleaved protein, but without GFP, therefore being 27 kDa smaller than the corresponding isoform in TACC3-GFP, which maintains the GFP tag on the C-terminal of the truncated protein. Further evaluation of the location of these cleavage sites and their possible regulation is warranted, and constitutes an ongoing phase of my research. One of the cleavage sites is probably located shortly upstream of the coiled-coil domains, within the highly conserved and phosphorylated domain (noted in Figure 9). Phosphorylation of certain sites here, most notably Serine 638 (found in a highly basic set of residues much like a thrombin cut site) may be what triggers proteolytic cleavage of TACC3 and the resultant effects on microtubule dynamics. Further mutagenesis experiments are being performed to create a construct lacking only this domain, to see if it can still be cleaved in the same way.

TACC3 also contains a number of conserved phosphorylation sites (Figure 14, yellow) and surrounding consensus sequences homologous to those characterized in human TACC3. I compiled information on these sites and the few studies characterizing them in *Xenopus*. These sites include several phosphorylated by Aurora A Kinase (AAK) (Serine 33, Serine 620, Serine 626) found to be relevant for TACC3's localization to the spindle apparatus in mitosis (Kinoshita *et al*., 2005). There are a number of other residues phosphorylated by Cdk1 (Threonine 58, Serine 152, Serine 311, Serine 343, Serine 451, Serine 638) to enable TACC3 to bind the translational regulator eIF4E and play a role in regulating translation of certain mRNAs (Barnard *et al*., 2005). These residues, and

others we found to be phosphorylated in TACC3 in collaboration with the Ballif lab at the University of Vermont (Serine 509, Threonine 562) were determined to be promising candidates to investigate. Phosphorylation of TACC3 on these specific sites is likely to be an important means of regulating TACC3's binding and possibly the proteolytic cleavage observed above. Each of these sites are described in the table below.

TACC3 Known Phosphorylated Sites

Xenopus site (Q9PTG8)	Human site (Q9Y6A5)	Kinase responsible	Homologous region?	Citation
Ser33	Ser34	AAK	Yes	Kinoshita 2005
Thr58	Thr59	Cdk1	Yes	Barnard 2005
Ser152	n/a	Cdk1	No	Barnard 2005
Ser311	Thr271	Cdk1	Yes	Barnard 2005
Ser343	Ser317	Cdk1	Yes	Barnard 2005
Ser451	Ser434	Cdk1	No	Barnard 2005
Ser509	Ser468	?	Yes	
Thr562	n/a	?	No	
Ser620	Ser552	AAK	Yes	Kinoshita 2005
Ser626	Ser558	AAK, PKA	Yes	Kinoshita 2005
Ser638	Ser570	Cdk1	Yes	Barnard 2005

To evaluate which sites were of the most significant interest, the sequence of *Xenopus* TACC3 surrounding the phosphorylated site was compared to the Human TACC3 sequence. If the *Xenopus* phosphorylated residue is still present and flanked by similar amino acids in Human TACC3, it was described as "homologous" in the table above and considered of greater interest, being evolutionarily conserved.

Several of these sites were chosen to selectively mutate to alanine residues, thereby blocking phosphorylation of that site without sterically affecting surrounding protein structures. I have tried to mutate Serines 311, 509, 626, and 638 and Threonine 562. These mutageneses have been successful so far with S311, T562, and S638, and I

will try again with the remaining sites. In the near future, localization experiments with these constructs should provide a clearer picture of the phosphorylation of TACC3 and its effects on TACC3's localization and overall structure.

TACC1 phosphorylation is also likely to be relevant to its +end localization. No studies on *Xenopus* TACC1 besides ours have ever been performed, however, so to begin to analyze TACC1 phosphorylation I had to first examine the little that is known about Human TACC1. Examination of a few studies (Olsen *et al.,* 2006; Gabillard *et al.,* 2011; Pu *et al.,* 2001) that characterized genome-wide phosphorylation found a number of sites phosphorylated in human TACC1 that are conserved in *Xenopus* TACC1. These are shown in the table below:

TACC1 Possible Phosphorylated Sites

***Xenopus* possible site**	Human TACC1 (O75410) site	Homologous region?	Citation
Ser4	Ser4	Yes	Olsen *et al.,* 2006
Ser10	Ser10	Yes	Olsen *et al.,* 2006
Ser50, Ser55, Ser57	Serine series: 50,52,54,55,57	Yes but 52+54 not present	Olsen *et al.,* 2006
Ser239	Ser228	Yes	Gabillard *et al.,* 2011
Tyr551	Tyr719*	Yes	Pu *et al.,* 2006

*Tyr719 is also homologous to Tyr821 in human TACC2 (O95359), also phosphorylated.

These sites represent possible targets for future studies of TACC1 phosphorylation and regulation. Of particular interest are Serine 239, known to be phosphorylated by Aurora C Kinase (Gabillard *et al.,* 2011) and Tyrosine 551, homologous not only to human TACC1 Tyr719 but also human TACC2 Tyr821, which is also phosphorylated. These tyrosines are present at what seems to be at or near the junction of the two coiled-coil domains of TACCs 1+2, and are within a set of residues not just homologous but identical to the *Xenopus* orthologs. I have planned out the

mutagenesis of these two sites in TACC1 and intend to create the mutant constructs for analysis shortly before leaving our lab. Future studies of these sites may reveal additional means of regulating the structure and function of the TACC family, and how this regulation may be critically important to the process of axon guidance and neurodevelopment as a whole.

Finally (and most obviously), our lab will also seek to clone and study TACC2 in the same manner as TACCs 1 and 3. It is clear that it is present in the *Xenopus* genome but no other studies have even begun to examine its expression and functions in this model organism. This thesis' investigations into the totally uncharacterized TACC1 gene, and it's further evaluations of the role of TACC3 in neurodevelopment have laid good methodological groundwork for this future series of experiments.

REFERENCES

Akhmanova A, Steinmetz MO (2008). Tracking the ends: a dynamic protein network controls the fate of microtubule tips. Nat Rev Mol Cell Biol 9, 309–322.

Applegate KT, Besson S, Matov A, Bagonis MH, Jaqaman K, Danuser G (2011). plusTipTracker: quantitative image analysis software for the measurement of microtubule dynamics. J Struct Biol 176, 168–184.

Barnard DC, Cao Q, Richter JD (2005). Differential phosphorylation controls Maskin association with eukaryotic translation initiation factor 4E and localization on the mitotic apparatus. Mol Cell Biol 25, 7605–7615.

Bellanger JM, Gonczy P (2003). TAC-1 and ZYG-9 form a complex that promotes microtubule assembly in C. elegans embryos. Curr Biol 13, 1488–1498.

Brouhard GJ, Stear JH, Noetzel TL, Al-Bassam J, Kinoshita K, Harrison SC, Howard J, Hyman AA (2008). XMAP215 is a processive microtubule polymerase. Cell 132, 79–88.

Buey R.M., Sen I., Kortt O., Mohan R., Gfeller D., Veprintsev D.,Kretzschmar I., Scheuermann J., Neri D., Zoete V. *et al*. (2012). Sequence determinants of a microtubule tip localization signal (MtLS). J. Biol. Chem.287, 28227-28242. doi:10.1074/jbc.M112.373928

Campbell, D.S. and C.E. Holt. Chemotropic responses of retinal growth cones mediated by rapid local protein synthesis and degradation.Neuron 32:1013-26 (2001).

Dwivedy A, Gertler FB, Miller J, Holt CE. (2007). Ena/VASP function in retinal axons is required for terminal arborization but not pathway navigation. Development134, 2137-2146.

Engle, EC. (2010). Human genetic disorders of axon guidance. *Cold Spring Harb Perspect Biol*. March; 2(3): a001784

Engel U, Zhan Y, Long JB, Boyle SN, Ballif BA, Dorey K, Gygi SP, Koleske AJ, Vanvactor D (2014). Abelson phosphorylation of CLASP2 modulates its association with microtubules and actin. Cytoskeleton (Hoboken) 71, 195–209.

Falk J, Drinjakovic J, Leung KM, Dwivedy A, Regan AG, Piper M, Holt CE (2007). Electroporation of cDNA/Morpholinos to targeted areas of embryonic CNS in *Xenopus*. BMC Developmental Biology 7:107.

Fu W., Chen H., Wang G., Luo J., Deng Z., Xin G., Xu N., Guo X., Lei J., Jiang Q. (2013). Self-assembly and sorting of acentrosomal microtubules by TACC3 facilitate kinetochore capture during the mitotic spindle assembly.Proc. Natl. Acad. Sci. USA 110, 15295–15300. doi:10.1073/pnas.1312382110

Gabillard JC, Ulisse S, Baldini E, Sorrenti S, Cremet JY, Coccaro C, Prigent C, D'Armiento M, Arlot-Bonnemains Y (2011). Aurora-C interacts with and phosphorylates the transforming acidic coiled-coil 1 protein. Biochem Biophys Res Common. 408(4):647-53

Gergely F, Karlsson C, Still I, Cowell J, Kilmartin J, Raff JW (2000a). The TACC domain identifies a family of centrosomal proteins that can interact with microtubules. Proc Natl Acad Sci USA 97, 14352–14357.

Gergely F, Kidd D, Jeffers K, Wakefield JG, Raff JW (2000b). D-TACC: a novel centrosomal protein required for normal spindle function in the early Drosophila embryo. EMBO J 19, 241–252.

Gutiérrez-Caballero, C., S.G. Burgess, R. Bayliss, and S.J. Royle. 2014. TACC3-ch-TOG track the growing tips of microtubules independently of clathrin and Aurora-A phosphorylation. Biology Open doi: 10.1242/bio.201410843

Ha, G.H., J.L. Kim, and E.K. Breuer. 2013. Transforming acidic coiled-coil proteins (TACCs) in human cancer. *Cancer letters*. 336:24-33.

Honnappa S, Gouveia SM, Weisbrich A, Damberger FF, Bhavesh NS, Jawhari H, Grigoriev I, van Rijssel FJ, Buey RM, Lawera A, *et al*. (2009). An EB1-binding motif acts as a microtubule tip localization signal. Cell 138, 366–376.

Holt CE (1989). A single-cell analysis of early retinal ganglion cell differentiation in Xenopus: from soma to axon tip. J Neurosci 9:3123–3145.

Hood F.E., Williams S.J., Burgess S.G., Richards M.W., Roth D., Straube A., Pfuhl M., Bayliss R., Royle S. J. (2013) Coordination of adjacent domains mediates TACC3-ch-TOG-clathrin assembly and mitotic spindle binding. J. Cell Biol. 202, 463–478

Hur EM, Saijilafu, Lee BD, Kim SJ, Xu WL, Zhou FQ (2011). GSK3 controls axon growth via CLASP-mediated regulation of growth cone microtubules. Genes Dev 25, 1968–1981.

Kinoshita K, Noetzel TL, Pelletier L, Mechtler K, Drechsel DN, Schwager A, Lee M, Raff JW, Hyman AA (2005). Aurora A phosphorylation of TACC3/ maskin is required for centrosome-dependent microtubule assembly in mitosis. J Cell Biol 170, 1047–1055.

Lauffart, B., A. Dimatteo, M.M. Vaughan, M.A. Cincotta, J.D. Black, and I.H. Still. 2006. Temporal and spatial expression of TACC1 in the mouse and human. *Developmental dynamics : an official publication of the American Association of Anatomists*. 235:1638-1647.

Lauffart, B., S.J. Howell, J.E. Tasch, J.K. Cowell, and I.H. Still. 2002. Interaction of the transforming acidic coiled-coil 1 (TACC1) protein with ch-TOG and GAS41/NuBI1

suggests multiple TACC1-containing protein complexes in human cells. *The Biochemical journal*. 363:195-200.

Le Bot N, Tsai MC, Andrews RK, Ahringer J (2003). TAC-1, a regulator of microtubule length in the C. elegans embryo. Curr Biol 13, 1499–1505.

Lee H, Engel U, Rusch J, Scherrer S, Sheard K, Van Vactor D (2004). The microtubule plus end tracking protein Orbit/MAST/CLASP acts downstream of the tyrosine kinase Abl in mediating axon guidance. Neuron 42, 913–926.

Lee MJ, Gergely F, Jeffers K, Peak-Chew SY, Raff JW (2001). Msps/ XMAP215 interacts with the centrosomal protein D-TACC to regulate microtubule behaviour. Nat Cell Biol 3, 643–649.

Leung, K-M., van Horck, FPG, Andrew C Lin, Allison, R., Standart, N. and Holt, CE. Asymmetrical b-actin mRNA translation in growth cones mediates attractive turning to netrin-1. Nature Neuroscience 9:1247-56 (2006).

Long JB, Bagonis M, Lowery LA, Lee H, Danuser G, Van Vactor D (2013). Multiparametric analysis of CLASP-interacting protein functions during interphase microtubule dynamics. Mol Cell Biol 33, 1528–1545.

Lowery LA, Stout A, Faris AE, Ding L, Baird MA, Davidson MW, Danuser G, Van Vactor D (2013). Growth cone-specific functions of XMAP215 in restricting microtubule dynamics and promoting axonal outgrowth. Neural Dev 8, 22.

Lowery LA, Van Vactor D (2009). The trip of the tip: understanding the growth cone machinery. Nat Rev Mol Cell Biol 10, 332–343.

Marx A, Godinez WJ, Tsimashchuk V, Bankhead P, Rohr K, Engel U (2013). Xenopus cytoplasmic linker-associated protein 1 (XCLASP1) promotes axon elongation and advance of pioneer microtubules. Mol Biol Cell 24, 1544–1558.

Maurer SP, Cade NI, Bohner G, Gustafsson N, Boutant E, Surrey T (2014). EB1 accelerates two conformational transitions important for microtubule maturation and dynamics. Curr Biol 24, 372–384.

Murray AJ, Tucker SJ, Shewan DA. (2009). cAMP-Dependent Axon Guidance Is Distinctly Regulated by Epac and Protein Kinase A. J Neurosci 29, 15434 –15444.

Nakamura S, Grigoriev I, Nogi T, Hamaji T, Cassimeris L, Mimori-Kiyosue Y (2012). Dissecting the nanoscale distributions and functions of microtubule-end-binding proteins EB1 and ch-TOG in interphase HeLa cells. PloS One 7, e51442.

Nieuwkoop PD, Faber J (1994). Normal Table of Xenopus Laevis (Daudin), New York: Garland.

Nwagbara, B.U., A.E. Faris, E.A. Bearce, B. Erdogan, P.T. Ebbert, M.F. Evans, E.L. Rutherford, T.B. Enzenbacher, and L.A. Lowery. 2014. TACC3 is a microtubule plus end-tracking protein that promotes axon elongation and also regulates microtubule plus end dynamics in multiple embryonic cell types. *Molecular biology of the cell*. 25:3350-3362.

O'Brien LL, Albee AJ, Liu L, Tao W, Dobrzyn P, Lizarraga SB, Wiese C (2005). The Xenopus TACC homologue, maskin, functions in mitotic spindle assembly. Mol Biol Cell 16, 2836–2847.

Olsen JV, Blagoev B, Gnad F, Macek B, Kumar C, Mortensen P, Mann M. (2006). Global, in vivo, and site-specific phosphorylation dynamics in signaling networks. Cell 127(3):635-48.

Peset I, Vernos I (2008). The TACC proteins: TACC-ling microtubule dynamics and centrosome function. Trends Cell Biol 18, 379–388.

Pu JJ, Li C, Rodiguez M, Banerjee D (2001). Cloning and sStructural Characterization of ECTACC, a New Member Of The Transforming Acidic Coiled Coil (TACC) Gene Family: cDNA Sequence and Expression Analysis in Human Microvascular Endothelial Cells. Cytokine 13(3), 129-137.

Sadek CM, Pelto-Huikko M, Tujague M, Steffensen KR, Wennerholm M, Gustafsson JA (2003). TACC3 expression is tightly regulated during early differentiation. Gene Expr Patterns 3, 203–211.

Shcherbo D, Murphy CS, Ermakova GV, Solovieva EA, Chepurnykh TV, Shcheglov AS, Verkhusha VV, Pletnev VZ, Hazelwood KL, Roche PM, *et al*. (2009). Far-red fluorescent tags for protein imaging in living tissues. Biochem J 418, 567–574.

Sive HL, Grainger RM, Harland RM (2010). Microinjection of Xenopus embryos. Cold Spring Harbor Protocols 2010, pdb.ip81.

Srayko M, Quintin S, Schwager A, Hyman AA (2003). Caenorhabditis elegans TAC-1 and ZYG-9 form a complex that is essential for long astral and spindle microtubules. Curr Biol 13, 1506–1511.

Still, I.H., M. Hamilton, P. Vince, A. Wolfman, and J.K. Cowell. 1999. Cloning of TACC1, an embryonically expressed, potentially transforming coiled coil containing gene, from the 8p11 breast cancer amplicon. *Oncogene*. 18:4032-4038.

Still IH, Vettaikkorumakankauv AK, DiMatteo A, Liang P. Structure-function evolution of the transforming acidic coiled coil genes revealed by analysis of phylogenetically diverse organisms. BMC Evol Biol. 2004 Jun 18;4:16.

Stout A, D'Amico S, Enzenbacher T, Ebbert P, Lowery LA (2014). Using plusTipTracker software to measure microtubule dynamics in Xenopus laevis growth cones. J Vis Exp, e52138.

Tanaka EM, Ho T, Kirschner MW (1995). The role of microtubule dynamics in growth cone motility and axonal growth. J Cell Biol 128, 139–155.

Tanaka EM, Kirschner MW (1991). Microtubule behavior in the growth cones of living neurons during axon elongation. J Cell Biol 115, 345–363.

Tessmar K, Loosli F, Wittbrodt J (2002). A screen for co-factors of Six3. Mech Dev 117, 103–113.

Thakur HC, Singh M, Nagel-Steger L, Kremer J, Prumbaum D, Fansa EK, Ezzahoini H, Nouri K, Gremer L, Abts A, *et al*. (2014). The centrosomal adaptor TACC3 and the microtubule polymerase chTOG interact via defined C-terminal subdomains in an Aurora-A kinase-independent manner. J Biol Chem 289, 74–88.

Tischfield MA, Baris HN, Wu C, *et al*. Human *TUBB3* mutations perturb microtubule dynamics, kinesin interactions, and axon guidance. *Cell*. 2010;140(1):74-87. doi:10.1016/j.cell.2009.12.011.

van Horck F.P., Weinl C., Holt C.E. Retinal axon guidance: novel mechanisms for steering. Curr. Opin. Neurobiol. 2004;14:61–66.

Xie Z, Moy LY, Sanada K, Zhou Y, Buchman JJ, Tsai LH (2007). Cep120 and TACCs control interkinetic nuclear migration and the neural progenitor pool. Neuron 56, 79–93.

Yang YT, Wang CL, Van Aelst L (2012). DOCK7 interacts with TACC3 to regulate interkinetic nuclear migration and cortical neurogenesis. Nat Neurosci 15, 1201–1210.

Zhou FQ, Zhou J, Dedhar S, Wu YH, Snider WD (2004). NGF-induced axon growth is mediated by localized inactivation of GSK-3beta and functions of the microtubule plus end binding protein APC. Neuron 42, 897–912.